



UNIVERSITÀ
DEGLI STUDI
FIRENZE

FLORE

Repository istituzionale dell'Università degli Studi di Firenze

Nanoparticles and organized lipid assemblies: from interaction to design of hybrid soft devices

Questa è la Versione finale referata (Post print/Accepted manuscript) della seguente pubblicazione:

Original Citation:

Nanoparticles and organized lipid assemblies: from interaction to design of hybrid soft devices / Marco Mendoza, Lucrezia Caselli, Annalisa Salvatore, Costanza Montis, Debora Berti. - In: SOFT MATTER. - ISSN 1744-6848. - STAMPA. - 15:(2019), pp. 8951-8970. [10.1039/C9SM01601E]

Availability:

This version is available at: 2158/1175074 since: 2022-06-01T15:59:52Z

Published version:

DOI: 10.1039/C9SM01601E

Terms of use:

Open Access

La pubblicazione è resa disponibile sotto le norme e i termini della licenza di deposito, secondo quanto stabilito dalla Policy per l'accesso aperto dell'Università degli Studi di Firenze (<https://www.sba.unifi.it/upload/policy-oa-2016-1.pdf>)

Publisher copyright claim:

(Article begins on next page)

REVIEW

Nanoparticles and organized lipid assemblies: from interaction to design of hybrid soft devices

Marco Mendoza, Lucrezia Caselli, Annalisa Salvatore, Costanza Montis* and Debora Berti*

Received 00th January 20xx,
Accepted 00th January 20xx

DOI: 10.1039/x0xx00000x

This contribution reviews the state of art on hybrid soft matter assemblies composed of inorganic nanoparticles (NP) and lamellar or non-lamellar lipid bilayers. After a short outline of the relevant energetic contributions, we address the interaction of NPs with synthetic lamellar bilayers, meant as cell membrane mimics. We then review the design of hybrid nanostructured materials composed of lipid bilayers and some classes of inorganic NPs, with particular emphasis on the effects on the amphiphilic phase diagram and on the additional properties contributed by the NPs. Then, we present the latest developments on the use of lipid bilayers as coating agents for inorganic NPs. Finally, we remark the main achievements of the last years and our vision for the development of the field.

1	1. Introduction	28	In this contribution, particular attention will be devoted to non-covalent interactions that take place when NPs and lipid bilayers are put into contact. Understanding the nature and the key determinants of these interactions is instrumental both for fundamental and applied soft matter research.
2		29	
3	Lipid bilayers are ubiquitous structural motifs in natural and synthetic soft matter assemblies. Their interaction with nanostructured matter, and in particular with nanoparticles (NPs), is therefore of interest both for natural and engineered systems. In addition, the shared length and energy scales, combined with the peculiar properties of inorganic matter at the nanoscale, can be harnessed to use NPs to probe selected physical properties of membranes or to modify the amphiphilic phase diagram under external <i>stimuli</i> .	30 31 32 33 34 35 36 37 38 39	This review is organized as follows: a short theoretical section will introduce the main energetic contributions at stake when NPs interact with lipid bilayers (section 2). Then, we will provide an overview of the most relevant studies which have recently addressed the interaction of NPs with synthetic phospholipid bilayers, meant as simplified and highly controllable mimics of cell membranes (section 3). In this section, we will emphasize some examples where the investigation on model systems contributed disclosing non-covalent interactions at play in living systems. Then, we will review (section 4) the design of hybrid nanostructured materials composed of lipid bilayers and inorganic nanoparticles, with particular emphasis on the effects on the amphiphilic phase diagram and on the additional properties contributed by the NPs. Then, we will present the latest developments on the use of lipid bilayers as coating agents for inorganic NPs (section 5), whose aim is the improvement of dispersibility, biocompatibility and pharmacokinetic properties. Finally, a conclusive paragraph will remark the main achievements of the last years and our vision for the development of the field.
12	In this contribution we will review the state of the art concerning research on hybrid soft matter assemblies composed of inorganic NPs and synthetic lipid bilayers, either in lamellar or non-lamellar arrangement.	40 41 42 43	
16	This topic is currently a very active area of research, with implications ranging from the design of smart nanostructured hybrid devices, where nanoparticles are included or functionalized with lipid bilayers, to the quest for mechanistic understanding of events taking place at the nano-bio-interface, relevant for nanomedicine and toxicity of nanomaterials.	44 45 46 47 48 49	
22	This review will focus on some selected classes of inorganic nanomaterials, namely metals (Au and Ag), metal oxides (like iron and zinc oxide) and silica NPs. The interaction of several other kinds of nanomaterials with lipid bilayers has been described in the literature and we refer the readers to some excellent recent reports on these topics ^{1–8} .	50 51 52 53 54 55 56 57	

Department of Chemistry "Ugo Schiff", University of Florence, and CSGI (Italian Center for Colloid and Surface Science, Via della Lastruccia 3, Sesto Fiorentino, 50019 Firenze.

Electronic Supplementary Information (ESI) available: [details of any supplementary information available should be included here]. See DOI: 10.1039/x0xx00000x

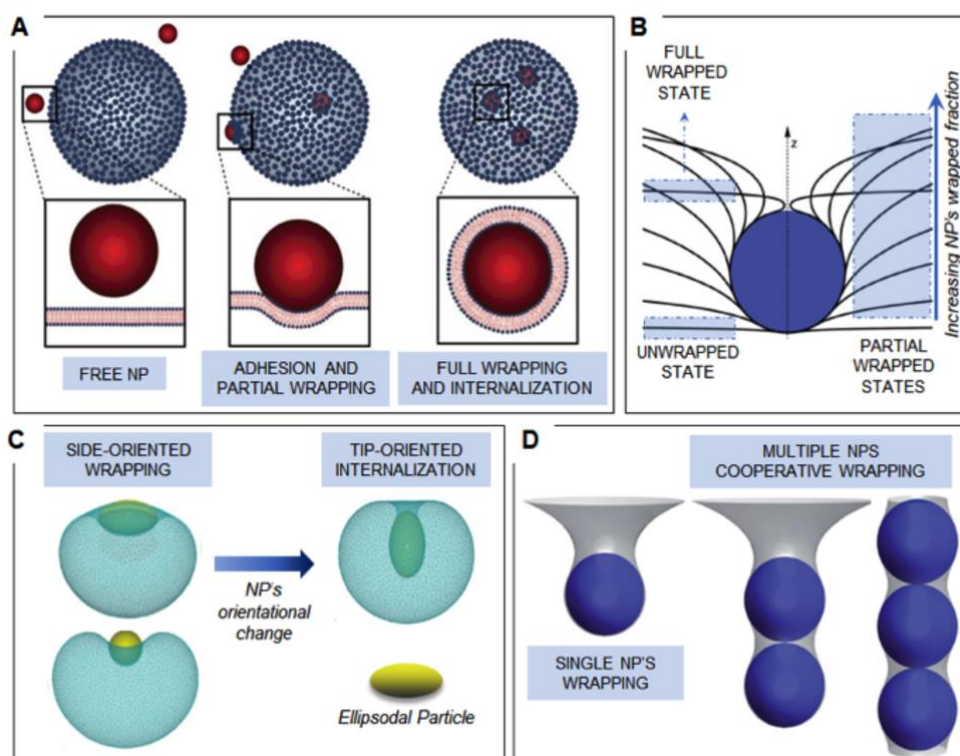


Figure 1 Theory of NPs-lipid membranes interactions. *Panel A* Illustration of the three possible configurations for a NP interacting with a lipid membrane: from left to right, (i) NP free in the environment (repulsive contribution to the NP-bilayer total interaction overcoming the attractive one), (ii) NP's adhesion to the membrane, causing NP's partial wrapping and (iii) NP's full engulfment (strong attractive NP-bilayer forces). Redapted from open access reference¹³. *Panel B* Illustrative picture representing unwrapped, fully wrapped and different wrapping degree-intermediate configurations for a NP interacting with a fluid interface. Reproduced from Ref.¹⁰¹ with permission from The Royal Society of Chemistry. *Panel C* Ellipsoidal NP's reorganization from a side-oriented configuration, adopted during the wrapping process, to a tip-oriented configuration, minimizing the energy required for full NP's engulfment and internalization. Reproduced from Ref.¹⁶ with permission from The Royal Society of Chemistry. *Panel D* Illustrative picture of (from left to right) a single NP wrapped by a fluid interface, two and three NPs wrapped in a membrane tube. Reproduced from Ref.¹⁰¹ with permission from The Royal Society of Chemistry.

2. Interaction of Nanoparticles with Lipid Membranes: the role of non-covalent forces

In this section we will consider the events following the exposure of a free-standing synthetic lipid bilayer to NPs, outlining the different contributions to the total interaction energy.

2.1 Theoretical description of NPs-lipid membrane interaction

The interaction between a NP and a lipid bilayer might lead to NP's adhesion on the bilayer, which can be followed by partial or total engulfment by the membrane. In a well-defined medium and at a given temperature, the NP docking to lipid membranes is thermodynamically favoured if the adhesion energy $E_{adh} < 0$, i.e., if the attractive terms overcome the repulsive ones. Considering a prototypical model of bioinorganic interface, with a spherical NP of radius R_1 interacting with a liposomal membrane with curvature $1/R_2$ the energetic balance between repulsive and attractive forces can be approximately described by a classical DLVO (Derjaguin-Landau-Verwey-Overbeek) formalism, as in eq. (1), including only the electrical double layer (E^{EL}) and the London-Van der Waals (E^{LW}) contributions to the total energy of adhesion:

$$E_{adh} = E^{EL} + E^{LW} \quad (1)$$

Where the terms E^{EL} , derived as a combination between the linear Debye-Huckel and the Derjaguin approximations and valid for surface potentials < 25 mV, and E^{LW} are described in eq. (2) and (3), respectively:

$$E^{EL} = \frac{\varepsilon R_1 R_2 (\psi_1^2 + \psi_2^2)}{4(R_1 + R_2)} \left[\frac{2\psi_1 \psi_2}{(\psi_1^2 + \psi_2^2)} \ln \left(\frac{1 + e^{-kd}}{1 - e^{-kd}} \right) + \ln(1 - e^{-2kd}) \right] \quad (2)$$

$$E^{LW} = -A \frac{R_1 R_2}{6(R_1 + R_2)} \left(\frac{1}{d} - \frac{1}{(d+h)} \right) - \frac{A}{6} \ln \left(\frac{d}{d+h} \right) \quad (3)$$

Where ψ_1^2 and ψ_2^2 are the surface potentials of the NP and the membrane, d the NP-membrane distance, k the Debye length, h the membrane's thickness, and A is the Hamaker constant. Although the DLVO theory generally succeeds in predicting the colloidal stability of hard colloids (e.g. inorganic NPs) suspended in a liquid medium, it often fails in describing the interaction of NPs with free-standing bilayers; a more comprehensive description for E_{adh} includes additional repulsive hydration forces establishing at short NPs-membrane distances, as well as hydrophobic NP-lipid chain attraction (the interested reader is referred to a recent report for the analytical expression of these two supplementary energetic contributions⁹).

Once the NP is adsorbed onto the lipid surface (i.e. $E_{adh} < 0$), the elastic properties of the membrane comes into play, and their balance with the adhesion forces determines the degree of

1 membrane deformation and NP's wrapping. Specifically, the
 2 energetic gain due to the adhesion forces is maximized by
 3 increasing the contact area between the NP and the lipid
 4 membrane, according to equation (4)¹⁰:

$$E_{adh} = -w \int_0^{S_{ad}} dS \quad (4)$$

5 with w adhesion energy per unit area and S_{ad} the contact area
 6 between the membrane and the NP. On the other side, the NP's
 7 wrapping is associated with a free energy cost of imposing
 8 membrane deformation (E_{el}), which is expressed through the
 9 Cahnam-Helfrich-Evans formalism¹⁰:

$$E_{el} = \int_0^S dS [\gamma + 2k_B(H - c_0)^2 + \bar{k}K] \quad (5)$$

12 with S the entire interfacial area.
 13 As we can see from eq. (5), the deformation penalty depends
 14 both on the membrane's topology, through the mean H and
 15 Gaussian K curvatures, and on the interface's mechanical and
 16 elastic properties, expressed by the surface tension γ , bending
 17 rigidity k_B , spontaneous curvature c_0 and Gaussian saddle splay
 18 modulus \bar{k} . It is the fine interplay between E_{adh} and E_{el} that
 19 ultimately defines the NP-membrane arrangement which
 20 minimizes the system's energy, ranging from completely
 21 unwrapped NPs (e.g. for small nanoparticles and/or weakly
 22 interacting with the lipid phase), to larger and/or strongly
 23 adhered nano-objects, eventually fully engulfed by the lipid
 24 membrane (See Figure 1A).

25 Based on the above treatment, we will now discuss the
 26 several NPs- and membrane-related factors implicated in this
 27 interaction, with particular attention on size, shape, surface
 28 coating of NPs and NP-NP correlations; on the "membrane"
 29 side, we will take into account some selected physicochemical
 30 properties and the zero or non-zero curvature.

31 Depending on their size, the adhesion of NPs on a target
 32 planar membrane can result in different effects: small NPs can
 33 either remain embedded in the lipid membrane or directly
 34 diffuse through it; relatively larger particles (>10 nm) can be
 35 wrapped by the membrane¹¹. This process is finely controlled
 36 by the energetic balance between the adhesion forces (eq. (4))
 37 and the membrane's elastic deformation penalty (eq.(5))
 38 leading to an optimal size for wrapping, as first observed by
 39 Roiter et al.¹². In particular, two characteristic NPs' limiting radii
 40 for a successful engulfment by lipid membranes can be
 41 theoretically predicted¹⁰:

$$R_{kw} = \sqrt{\frac{2k_b}{E_{adh}}} \quad (6)$$

$$R_{ky} = \sqrt{\frac{2k_b}{E_{adh} - \gamma}} \quad (7)$$

44 Within the bending-dominated regime (i.e. for relatively small
 45 membrane's deformation), the membrane tension can be
 46 neglected, and the wrapping process is mainly controlled by the
 47 competition between membrane's bending and NP's adhesion

strength, defining a critical radius R_{kw} . NPs with $R < R_{kw}$
 remain unwrapped, while larger NPs ($R > R_{kw}$) are fully
 engulfed inside the lipid scaffold. For larger membrane's
 deformation (e.g. induced by micron-sized particles), a
 characteristic length scale $\lambda = (2k_b/\gamma)^{1/2}$, which depends
 solely on membrane's properties, marks the crossover from the
 bending-dominated to the stretching-dominated regime^{9,13}
 (Figure 1 B), where the γ -dependent wrapping extent gradually
 increases with NP's size. The full engulfment is reached for a
 second crossover NP's radius R_{ky} (eq. (7)), representing a larger
 NP's limiting size, which is required for the internalization in the
 case of finite tension-membranes.

2.2 Key NPs features in the interaction with lipid membranes

Concerning NPs shape, the increase of the surface
 area/volume ratio from spherical to asymmetrical NPs (e.g.
 nanorods, nanoprisms and nanocubes), maximizes the surface
 available for absorption onto lipid membranes (eq. (4)),
 enhancing their reactivity¹⁴; on the other side, the local
 particle's surface curvature is predicted to increase the energy
 barrier associated to membrane's deformation, stabilizing
 partial-wrapping states also for tensionless membranes^{9,10}.
 Moreover, the interaction of asymmetric NPs with target lipid
 membranes can lead to preferential wrapping orientations, to
 minimize the energy cost for wrapping^{15,16} (See Figure 1C).
 Eventually, the asymmetric shape of NPs can drive peculiar self-
 assembly phenomena at the nano-bio interface, some examples
 of which are given in Section 3.

The NPs surface functionalization represents another
 important factor affecting the interaction with membranes; in
 particular, NPs surface charge has a major impact on adhesion
 both onto charged and zwitterionic interfaces, setting the sign
 and magnitude of the electrostatic long-range contribution of
 (eq.1)^{3,17-21}. Furthermore, the adhesion of charged NPs to a
 target membrane is also associated to an entropic gain, deriving
 from the release of small counterions from the NP surface²²
 (See Figure 1D). On the other side, the presence of polymeric
 steric stabilizers on the NPs surface, like for PEGylated particles,
 often decreases the adhesion energy; this effect can be
 understood considering the mobility loss experienced by the
 polymer chains approaching the lipid surface, which entails a
 considerable entropic penalty for membrane adhesion.
 Moreover, NPs' surface functionalization determines their
 polarity, which is key in controlling their spontaneous
 localization when challenging a free-standing lipid membrane:
 generally, hydrophilic nanomaterials with size larger than 10 nm
 reside at the membrane surface, with the possibility to be
 partially or fully wrapped by the membrane. Conversely,
 depending on their hydrophobicity²³, small particles can either
 spontaneously cross^{24,25} or be entrapped²⁴ within the lipid
 membrane, provoking an alteration of the bilayer's frustration
 packing energy²⁶⁻³¹.

Eventually, interparticle forces between different membrane-
 bound NPs may originate cooperative phenomena, ultimately
 leading to the simultaneous wrapping and engulfment of

1 multiple NPs (see Figure 1D), which will be discussed in detail 56
 2 section 3. 57

4 2.3 Key membrane features in the interaction with NPs 58

5 Membrane-related characteristics have a crucial role in the 59
 6 interaction with NPs. In particular, the composition of lipid 60
 7 bilayers determines specific physico-chemical, viscoelastic and 61
 8 thermodynamic properties of relevance in the interaction with 62
 9 NPs. Membrane's surface potential, determined by the 63
 10 percentage of non-ionic, anionic and cationic lipids, strongly 64
 11 affects the electrostatic contribution to NPs adhesion (eq. 10) 65
 12 while the presence of specific components (e.g. cholesterol) 66
 13 and their relative abundance, give rise to characteristic 67
 14 behaviours, which will be extensively discussed in section 3. 68

15 Equally important, the molecular geometry of the 69
 16 membrane's components determines the equilibrium 70
 17 arrangement of lipids within the bilayer. The molecular packing 71
 18 represents the main factor affecting both the physical state and 72
 19 the overall topological curvature of membranes, which are two 73
 20 prominent determinants in the interactions with 74
 21 nanomaterials. 75

22 In particular, the interactions at the nano-lipid interface 76
 23 are extremely affected by the gel-liquid crystalline phase behaviour 77
 24 of lipid membranes: by increasing temperature, lipid bilayers 78
 25 undergo a main phase transition from the so-called "gel state" 79
 26 (L_{β}), where hydrocarbon chains are tightly packed and almost 80
 27 locked in place, to a "fluid state" (L_{α}), where lipids freely diffuse 81
 28 within the 2D membrane's plane. The "melting transition 82
 29 temperature" (T_m) is specific for a given lipid composition and 83
 30 determines the elastic response of membranes at a given 84
 31 temperature. In particular, gel phase bilayers show a reduced 85
 32 reactivity with nanomaterials, mostly due to the high value of 86
 33 their bending rigidity (k_B) with respect to the fluid phase 87
 34 which strongly hampers the membrane's bending and wrapping 88
 35 around NPs (see eq. (5-7)). On the other side, the interaction 89
 36 with NPs, which can proceed through polar headgroups 90
 37 (hydrophilic NPs) or hydrophobic chains (hydrophobic NPs) 91
 38 might affect the lipid molecular packing, leading to micro 92
 39 and macroscopic modifications in the membrane structure and 93
 40 thermotropic behaviour (specific examples will be provided in 94
 41 the following paragraphs).

42 As predicted from eq.5, the membrane's topology plays a 95
 43 crucial role in its elastic response to NP's induced deformations. 96
 44 Although lipid membranes are generally visualized as flat 97
 45 bilayers (H and G in eq. (5) equal to zero), both biomembranes 98
 46 and synthetic lipid assemblies may fold into more organized 99
 47 non-lamellar bilayered structures³². The interaction of 100
 48 nanomaterials with such non-lamellar structures may have a 101
 49 noteworthy relevance both for biomimetic and technological 102
 50 applications^{33,34}, (as discussed in details in the following 103
 51 paragraphs) while it remains, to date, a highly unexplored 104
 52 research area.

53 Differently from planar membranes, curved membranes are 105
 54 defined by positive (direct phases) or negative (inverse phases) 106
 55 mean curvature (H) and non-zero Gaussian curvature (K)³⁵ in

each point of their surface, with H and G described by eq. 8 and 9, respectively:

$$H = \frac{1}{2}(c_1 + c_2) \quad (8)$$

$$K = c_1 c_2 \quad (9)$$

with c_1 and c_2 minimum and maximum values of curvature at a specific point of membrane surface.

The non-zero values of H and K lead, as predicted from eq. (5), to a modification of their Helfrich energy and elastic response towards externally induced deformations (e.g. NPs' wrapping) with respect to the case of lamellar membranes. Moreover, different topologies are associated with a frustration packing free energy (E_P), which varies according to eq. (10)³⁶:

$$E_P = k(l - l_r)^2 \quad (10)$$

with k stretching rigidity of lipid chains, l and l_r hydrophobic chain extension in the stretched and relaxed state, respectively. Phase transitions between different geometries, including changes in both elastic and frustration packing energies, have high biological relevance, sharing similar energy barriers and molecular re-arrangements with membrane fusion processes³⁷. Several recent studies, which will be addressed in section 4, demonstrated that both hydrophilic and hydrophobic NPs can promote phase transitions between model mesophases with different geometry^{26,27,34,37-41}, lowering the energy barrier required to switch from low to high curvature phases. One of the first attempts to elucidate this effect is represented by recent works^{26,42}, where the transition temperature from cubic to hexagonal phases in monoolein liquid crystals is demonstrated to be finely controlled by inclusion of hydrophobic iron oxide NPs (see section 4). This behaviour was explained by combining the Helfrich theory in eq. (5) with geometrical considerations: NPs increase the frustration packing energy of the cubic phase (eq. (10)), while they have a milder effect on the hexagonal arrangement, by inserting into its hydrophobic voids (See Figure 2).

In the framework of this theoretical description, in recent years the interaction of NPs with lipid membranes has been

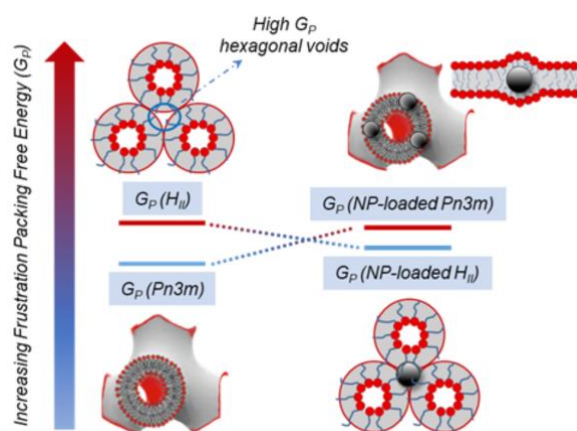


Figure 2 Effects of NPs on lipid mesophases architectures. Illustrative scheme of the NP-induced modification of the Frustration Packing Energy of both cubic and hexagonal mesophases.

1 explored with different approaches and for different purposes⁵⁴
 2 from fundamental studies employing lipid bilayers⁵⁵
 3 biomimetic platforms of tuneable physicochemical feature⁵⁶
 4 investigating the interaction with prototypical nanoparticles⁵⁷
 5 aimed at a better understanding of the efficiency and possible⁵⁸
 6 adverse effects of nanomaterials designed for biomedical⁵⁹
 7 applications, to applicative studies, where the interaction⁶⁰
 8 NPs and lipid membranes is exploited for analytical purposes⁶¹
 9 from the engineering of lipid assemblies with NPs inclusion,⁶²
 10 order to form smart hybrid materials for applications⁶³
 11 materials science, to the functionalization of NPs with a lipid⁶⁴
 12 coating, to improve their biocompatibility and pharmacokinetic⁶⁵
 13 properties.⁶⁶
 14 In section 3 we will review the interaction of NPs with⁶⁷
 15 synthetic lipid bilayers, taken as simplified models of real⁶⁸
 16 plasma membranes: in line with section 2, we will consider the⁶⁹
 17 main physicochemical factors, either related to NPs or to the⁷⁰
 18 lipid membrane, affecting the interaction under simplified⁷¹
 19 conditions. We will provide relevant examples from the recent⁷²
 20 literature, highlighting the connections, whenever they are⁷³
 21 relevant, between the findings on cell models and the *in vitro*/⁷⁴
 22 *vivo* observations.⁷⁵

23 3. NPs/biomembrane Interactions: from 24 biophysical studies of nano-bio interfaces to 25 applications

26 One of the main issues limiting the development⁷⁶
 27 nanomedicine and the translation of engineered nanomaterials⁷⁷
 28 into medical practice, is the poor understanding of their fate in⁷⁸
 29 biological fluids, and their short-term and long-term possible⁷⁹
 30 adverse cytotoxic effects^{37,43–49}. Recent reports have also⁸⁰
 31 highlighted how nanodevices designed for nanomedicine⁸¹
 32 applications, whose functionality/efficiency has been proved⁸²
 33 the lab-scale, completely fail reaching their biological targets⁸³
 34 once in a living organism⁵⁰. As a matter of fact, to date, nano⁸⁴
 35 therapeutics available on the market are mainly limited to⁸⁵
 36 polymeric- and liposomal-based formulations^{51,52}, while, apart⁸⁶
 37 from some iron oxide NPs-based formulations, inorganic and⁸⁷
 38 metallic particles are at research stage or in clinical trials⁸⁸
 39 With the ultimate aim to fill the gap between the⁸⁹
 40 design/synthesis/development of nanomaterials for⁹⁰
 41 nanomedicine and their end use application, it is necessary to⁹¹
 42 improve our fundamental knowledge on the interaction of⁹²
 43 nanomaterials with biologically relevant interfaces, particularly⁹³
 44 cell membranes.⁹⁴

45 Plasma membrane, primarily composed by a mixed⁹⁵
 46 phospholipid bilayer with embedded proteins, protects the⁹⁶
 47 interior and ensures its communication with the external⁹⁷
 48 environment. The mechanisms of cell signalling processes⁹⁸
 49 extremely complex and length scale-dependent, with small⁹⁹
 50 molecules spontaneously crossing the lipid barrier and large¹⁰⁰
 51 and/or polar molecules harnessing protein-mediated¹⁰¹
 52 transportations across the membrane¹³. The nanoscale, shared¹⁰²
 53 by engineered particles and biologically relevant¹⁰³

macromolecules (i.e., DNA, viruses, surface proteins), is mostly
 associated with endocytic pathways, where the internalisation
 of nano-objects is generally controlled by the membrane
 through specific receptor-protein binding for the case of
 biological species^{54,55}. However, it has been demonstrated that
 synthetic NPs can be wrapped and internalized by both model
 and real cell membranes in the absence of any receptor-
 mediated interaction^{43,55,56}, under exclusive control of non-
 specific interactions taking place at the nano-bio interface, and
 membrane's elasticity.

In this context, synthetic lipid membranes (together with
 more complex systems, as organ-on-a-chip and 3D cells arrays,
 mimicking an entire tissue⁵⁷), are interesting biomimetic
 systems, which, by mimicking the main structural unit of plasma
 membranes, allow investigating phenomena at the nano-bio
 interface in simplified and highly controlled conditions^{44,45,58}.

In recent years, both experimental and theoretical studies
 have addressed the interaction of NPs with synthetic lipid
 membranes, aimed at establishing clear connections between
 the results in simplified model systems and what observed in
 real cells, in order to enabling predictive strategies for the
 design of evermore efficient and non-toxic nanomaterials for
 nanomedicine.

In the following sections recent relevant studies on NPs-
 synthetic lipid membranes interactions, together with their
 implications for the understanding of real nano-bio interfaces,
 will be revised, particularly focusing on: the effect of NPs
 coating (surface charge, exchangeability of the ligand, steric
 hindrance of the coating, impact of the protein corona) (3.1);
 the effect of NPs size and shape (with particular interest on the
 relevance of NPs clusterization in cell uptake) (3.2); the effect of
 NPs adhesion on the composition, integrity and viscoelastic
 properties of the target membrane (3.3). In addition, the
 interaction of inorganic NPs and lipid membranes has been
 exploited for analytical purposes, in order to label/signal/probe
 selected properties of cells or lipid assemblies in complex
 biological media, both exploiting specific and non-specific
 interactions of NPs with the target membranes. This latter
 research field will be reviewed in section 3.4.

3.1 Biophysics of nano-bio interfaces: NPs coating

3.1.1 NPs surface charge

The intrinsic characteristics of NPs (i.e., core composition, size,
 shape) often have a secondary impact on the interaction with a
 target lipid membrane, which is primarily mediated by the ligands
 coating the NP's surface: the surface characteristics of NPs
 determine polarity and interfacial properties, directly involved in the
 electrostatic and London-Van der Waals contributions to NPs'
 adhesion to a lipid interface (see paragraph 2.1 for the theoretical
 background). The interaction of NPs with target membranes is
 primarily affect by the charge of both components (see equation 2).
 In order to closely resemble real plasma membranes, most of the
 employed model bilayers in biomimetics are characterized by a
 zwitterionic or slightly anionic nature. Therefore, negatively
 charged NPs tend to be electrostatically repelled from the

1 membrane, undergoing to weaker interactions with respect to
 2 cationic ones: remarkably, this is also observed for real cell
 3 membranes, where the uptake is generally much lower for
 4 anionic NPs than for cationic ones^{59–61}. However, the situation
 5 of real cells is complicated by the presence of other interaction
 6 pathways of specific nature, representing an alternative with
 7 respect to non-specific forces. Several studies have highlighted
 8 that nonionic, anionic and cationic NPs of similar sizes undergo
 9 different internalization routes, from clathrin- or caveola-
 10 mediated endocytosis to non-endocytic pathways, like passive
 11 diffusion^{62,63}. Even if characterized by limited interaction
 12 capability, yet anionic NPs are attractive for biomedical
 13 applications, due to limited adverse cytotoxic effects.
 14 In addition, despite the dominantly repulsive electrostatic forces,
 15 several reports have shown successful internalization of anionic
 16 NPs, as silica or Gold NPs (AuNPs)^{63–65}. Conversely, cationic NPs
 17 have a strong tendency to interact with negatively charged

membranes: it has been shown that cationic NPs adhere and
 clusterize onto synthetic target membranes, extract lipids from
 the membrane, ultimately provoking localized membrane
 disruption or integrity loss^{22,66,67}. In line with this findings, they
 are often characterized by limited stability in biological media
 and, above all, relevant toxic effects on real cells^{13,68,69}.
 Recently, Lee et al.⁷⁰ hypothesized, by means of a systematic
 study using a charge library of modified AuNPs, that the
 magnitude of the positive charge is not the sole factor
 determining the extent of interaction with target membranes
 and, thereby cytotoxicity. They conclude that spatial proximity
 of positively charged functional groups within a hydrophobic
 moiety is a common characteristic of toxic gold colloids.

3.1.2 NPs coated with steric stabilizers

A common strategy to increase the colloidal stability of NPs in
 biological media consists in the passivation of NPs with bulky
 ligands, to endow them with steric stabilization. This kind of
 coating also improves the pharmacokinetic properties of NPs:
 For instance, it is well known that PEGylation prevents
 opsonisation, improving the circulation time of the
 nanomaterial. This stealth effect of PEG in preventing
 opsonisation depends on its steric hindrance: it has been shown
 that both NPs uptake and circulation time depend on the
 molecular weight of PEG coating the NPs⁷¹. Moreover, thanks to
 molecular dynamic simulations, Lin et al.⁷² elucidated the effect
 of both the grafting density and polymer's chain length on the
 shielding ability of PEG layers bounded to gold NPs of varying
 size. Similar examples of steric stabilization of NPs have recently
 been proposed by Jiang and co-workers, who have employed
 poly(zwitterionic)protein functionalization (for instance
 poly(carboxybetaine)) to improve pharmacokinetic properties
 of NPs^{73,74}, while other examples of polyzwitterionic coatings
 are poly(acrylic acid) derivatives, poly(maleic anhydride-alt-1-
 alkene) derivatives or poly(sulfobetaine) derivatives, which
 offer several advantages over PEGylation (see as a reference the
 Review from Garcia et al.⁷³).

PEGylation or steric stabilization affects the interaction of NPs
 with synthetic target membranes, with possible implications
 also at the real membranes' level. Indeed, the use of steric
 stabilizers, like PEG, is theoretically predicted to decrease the
 adhesion of NPs to lipid membranes, due to the high entropic
 loss associated to the adsorption process (see paragraph 2).

Through large scale molecular dynamic simulations, In a recent
 study⁷⁵, Gal and coworkers extensively characterized the
 interaction of PEGylated SPIONs of different size with both
 synthetic membranes of different composition and real cancer
 and kidney cells. In the frame of classic DLVO theory (paragraph
 2), they presented a direct comparison of NP-synthetic and real
 membrane interactions, linking weak NP adsorption to anionic
 lipid membranes, due to NP-bilayer electrostatic interactions,
 with eukaryote cell uptake, without membrane penetration.
 Moreover, they showed that the NP-membrane electrostatic

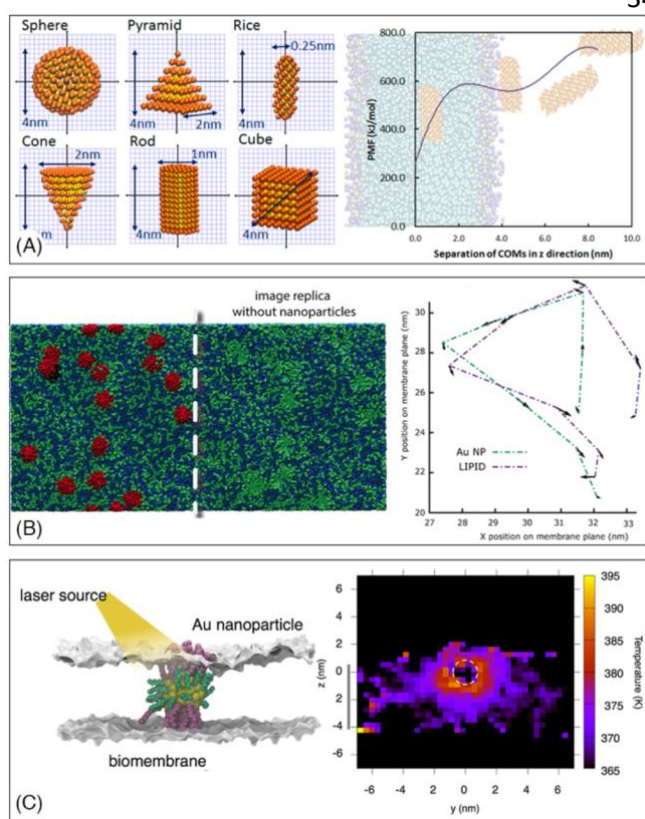


Figure 3 Theoretical studies on nano-bio interfaces. *Panel (A)* Molecular dynamics study to compute translocation rate constants of NPs of different shapes through lipid membranes; (left) coarse-grained gold nanoparticles setup; (right) analysis of rice NP translocation: potential of mean force, PMF (kJ/mol) profile as a function of distance of the NP from the lipid bilayer. Adapted with permission from¹⁰⁴. Copyright (2012) American Chemical Society. *Panel (B)* Lipid membrane modifications upon interaction with cationic gold NPs: (left) Lateral phase separation of 1:1 anionic (green) and zwitterionic (blue) lipids in the presence of gold NPs (red); (right) trajectories of NP (green) and anionic lipid (blue) highlighting the slaved diffusion of anionic lipids upon interaction with NPs. Adapted with permission from²². Copyright (2019) American Chemical Society. *Panel (C)* Nonequilibrium molecular dynamics simulations to investigate photoporation of lipid membranes through the irradiation of AuNPs: the NPs, stably bound to cell membranes, convert the radiation into heat; a quantitative prediction of the temperature gradient around the NP upon irradiation is evaluated. Adapted with permission from¹⁹⁷ Copyright (2017) American Chemical Society.

1 attraction is suppressed by increasing PEG molecular weight
 2 and NP size, which they correlated with low cell uptake and
 3 cytotoxicity in two cell lines.
 4 A common strategy to circumvent the poor ability of steri-
 5 stabilized NPs to interact with cells *via* non-specific interactions,
 6 limiting their cell uptake and therapeutic/diagnostic efficiency,
 7 is to exploit exploiting NP-membrane specific interactions
 8 which are available for the case of real plasma membranes.
 9 Endowing NPs surface with targeting moieties, might result in
 10 promoting the effective docking of NPs on cell membranes and
 11 improving the successful achievement of their biological target.
 12 For instance, in a proof-of-concept study it was shown that
 13 adding biotin or streptavidin moieties allows specific binding of
 14 polymer-coated NPs to beads carrying the complementary
 15 unit⁷⁶; Kaaki et al.⁷⁷ highlighted the efficient targeting of human
 16 breast carcinoma cells by folic acid-conjugated iron oxide NPs
 17 with a PEG coating; however, partially contradictory
 18 results were obtained by Kraus et al. on similar system, where
 19 folate-dependent targeting was highlighted⁷⁸

3.1.3 NPs coating with exchangeable ligands

22 The binding mode and strength between the NPs and the
 23 coating agent determine both single NP-membrane interactions
 24 and collective NP-NP interactions at the nano-bio interface.
 25 Physisorbed ligands, which can be easily displaced from the
 26 NP's surface through ligand-exchange, are associated to
 27 enhanced reactivity of NPs, which can be considered as
 28 "naked". Recently, hydrophobic physisorbed ligands, i.e. oleic
 29 acid/oleylamine coatings on iron oxide NPs, have been
 30 associated to small NPs' pearl-necklace aggregation inside
 31 monoolein bilayers²⁶. Moreover it has been shown that
 32 hydrophilic weakly adsorbed ligands on the surface of Au NPs
 33 can promote peculiar aggregation phenomena occurring on the
 34 lipid membrane^{18,19}, which are particularly significant also for
 35 the case of repulsive NPs/membrane electrostatic interactions
 36 (e.g. between negatively charged gold NPs and slightly anionic
 37 synthetic free-standing bilayers). Moreover, weakly bound
 38 physisorbed ligand onto the NPs surface can be easily replaced
 39 with other molecules establishing covalent or stronger non-
 40 specific interaction with the bare NPs surface: remarkably, it has
 41 been recently demonstrated by Wang et al.⁷⁹, that weak ligands
 42 as citrate and short DNA fragments onto the gold surface, can
 43 be effectively replaced with lipid components of cell
 44 membranes, resulting in unique interfacial phenomena. Indeed
 45 when ligand exchange processes occur at the interface, NPs
 46 might aggregate into ordered monolayers on the lipid
 47 membrane, which might affect membrane integrity and
 48 internalization efficiency and pathway.

3.1.4 Protein corona coating of NPs

51 An interesting aspect is the functionalization of NPs surface
 52 with the so-called protein corona^{14,55,80,81}. From the pioneer
 53 studies of K. Dawson⁸²⁻⁸⁴ and coauthors, it has been
 54 progressively established that NPs in biological fluids are
 55 spontaneously covered by a self-assembled layer of proteins
 56 inner non-exchangeable layer and an external exchangeable

one), which determines a "biological identity" of the NPs and,
 ultimately, their ability to interact with cells^{44,80,85,86}. The
 composition of the protein corona depends on the nature of
 NPs core, on their shape and on their surface coating. In
 particular, the surface charge of NPs also affects the adhesion
 of biomolecules present in biological media, modifying the
 protein corona, in terms of composition and orientation^{62,87,88}.
 It has also been highlighted that during NPs internalization, the
 tendency of corona proteins is, at least partially, to remain
 attached to NPs surface^{83,89,90}. Since proteins are generally
 characterized by significant steric hindrance and amphiphilic
 nature, they specifically mediate the interaction of the NPs with
 plasma membranes. In this context, it has been highlighted that
 slight physicochemical modifications of the proteins modify
 their binding and orientation on NPs, strongly affecting the
 biological uptake of NPs⁹¹. Recently, the controlled formation of
 the protein corona has been exploited both for application
 purposes (e.g., for applications in cancer vaccines⁹²) and also to
 control in a predictable way the protein-corona-mediated
 interaction of NPs with cell membranes. For instance, pre-
 incubation of NPs with serum has been exploited to prevent NPs
 aggregation in biological media, improve their cell uptake and
 decrease their cytotoxic effects⁶⁹. The comprehension, control
 and exploitation of protein corona formation is therefore a key
 milestone in determining and predicting NPs fate in living
 organisms.

3.2 Biophysics of nano-bio interfaces: NPs size and shape

As discussed in section 2, when a NP adheres to a planar lipid
 membrane, it locally imposes a curvature modification, which
 depends on the size of NPs and on the viscoelastic properties of the
 membrane (equation 5), which eventually controls the occurrence
 and extent of NPs wrapping by the membrane; therefore, NPs size
 also determines the response of the bilayer to its adhesion and,
 ultimately, the effects on the target membrane and the
 internalization pathway. NPs with size comparable or smaller than
 the lipid bilayer thickness can either be entrapped within the
 membrane³⁰ or translocate across the lipid bilayer by diffusing
 through^{25,93,94} or by opening pores in the membrane⁹⁵, which is
 normally associated to a high cytotoxicity *in vivo*^{56,96}. On the
 contrary, wrapping represents the dominant mechanism for larger
 particles (>10 nm) interacting with bilayers, which is associated to
 their entrance into cells in living organisms¹¹. Often, depending on
 NPs size, adhesion to a target membrane might result in the NPs
 clusterization: indeed, under specific conditions, membranes actively
 drive the self-assembly of adsorbed NPs, as a result of the tendency
 of the membrane to minimize the NP-induced deformation and its
 associated elastic cost (eq. 5)⁹⁷. As a result, small-sized NPs have
 been observed to preferentially interact with membranes as
 clusters^{67,98}, while fluid membranes have been theoretically
 predicted to mediate the asymmetric aggregation of spherical
 nanoparticles onto lipid surface⁹⁹. This aspect is particularly
 significant for medical application of nanomaterials, since NPs
 uptake in model and real membranes is often preceded by
 aggregation at the nano-bio interface¹¹. In addition, mathematical
 models and molecular dynamic simulations have revealed that
 membrane-induced interactions between bound particles can lead

1 to collective NPs wrapping and internalization: in particular, Zhang ²⁶
 2 al.¹⁰⁰ revealed that NPs translocation proceeds in a cooperative way ²⁷
 3 with a key role played by NPs quantity, while Lipowsky et al.^{101,28}
 4 showed that spherical NPs can be cooperatively wrapped in tubular ²⁹
 5 membrane invaginations. ³⁰
 6 While the effect of NP's size has been extensively investigated, ³¹
 7 much less is known on the impact of NP's geometry. Asymmetrically ³²
 8 shaped NPs, like nanorods, nanodisks and nanostars, are particularly ³³
 9 attractive materials, due to the peculiar properties (optical, ³⁴
 10 magnetic, electronic and so on) arising from anisotropy. ³⁵
 11 Depending on their shape, anisotropic NPs can efficiently interact ³⁶
 12 with a target membrane and translocate across it. MD studies on the ³⁷
 13 interaction of NPs of different non-spherical shapes highlighted ³⁸
 14 reorientation of NPs in proximity to the target membrane, to ³⁹
 15 maximize the interaction, leading to strong shape and orientational ⁴⁰
 16 dependence on the translocation¹⁰⁴ (See Figure 3A); in addition, it ⁴¹
 17 has to be considered that, from a theoretical standpoint, it ⁴²
 18 thermodynamically more favourable for a lipid membrane to wrap a ⁴³
 19 spherocylinder than a sphere of the same radius.¹⁰⁵ Consistently with ⁴⁴
 20 the theoretical predictions, non-spherical NPs, from nanostars to ⁴⁵
 21 nanorods, are efficiently internalized by cells, in a shape and, for ⁴⁶
 22 nanorods, aspect-ratio dependent manner.^{106,107} Experimental ⁴⁷
 23 studies on biomimetic membranes have shown that the asymmetric ⁴⁸
 24 shape of NPs can drive peculiar self-assembly phenomena at the ⁴⁹
 25 nano-bio interface^{10,37}: as an example, we recently demonstrated

that gold nanorods (Au NRs) are wrapped by model and real cell membranes as end-to-end NPs' clusters⁶⁷, reducing the energy penalty required for the membrane to bend around highly curved edges. The induced tension due to the adhesion of asymmetric NPs determines effects of lipid extraction, observed both on model membranes and macrophage cells, eventually provoking extensive disruption of the membrane, related to a significant *in vitro* cytotoxicity⁶⁷.

3.3 Biophysics of nano-bio interfaces: Membrane composition

Cell membranes are characterized by a high degree of compositional heterogeneity, typically comprising of thousands of different lipids, carbohydrates and proteins¹⁰⁸, which is reproduced, at different complexity levels, by model membranes. The chemical composition of both synthetic and natural bilayers strongly affects their elasticity, physical state and structure, thereby determining their response towards external *stimuli*. A clear example is the recent work of Lunnoo et al.¹⁰⁹, in which model bilayers with different compositional complexity levels correspond, as predicted by their proposed MD simulations, to diverse cellular uptake pathways of neutral 10-nm gold NPs. Going more into details, the presence of charges on the lipid membrane emphasizes the interaction with oppositely charged particles, as expected from eq. (2)⁹⁶ in

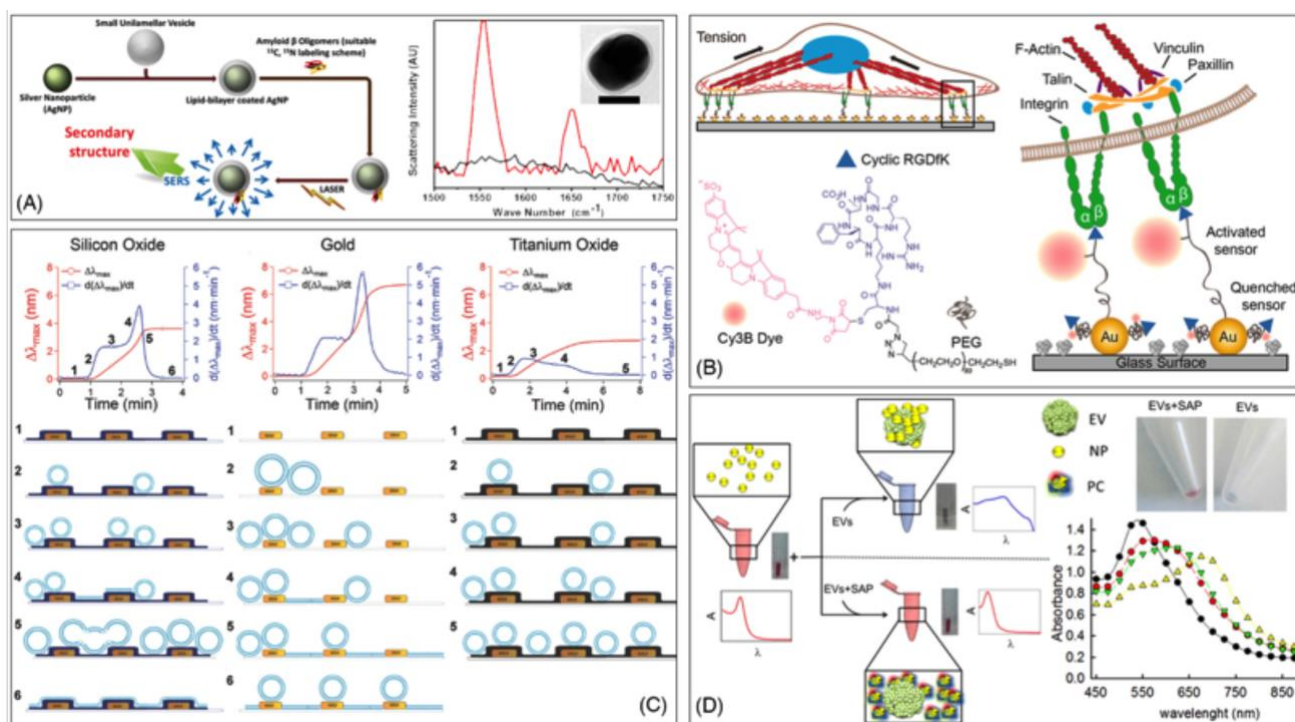


Figure 4 Analytical applications of NP-lipid membrane interactions. Panel (A) SERS technique exploiting the spontaneous binding of proteins to lipid bilayer-encapsulated AgNPs to probe lipid membrane-attached oligomers; (left) set-up of the technique (right) TEM micrograph of lipid-coated AgNPs; SERS spectrum of melittin in the presence of AgNPs (black) and lipid-coated AgNPs (red). Adapted with permission from¹²⁷. Copyright (2015) American Chemical Society. Panel (B) Molecular tension fluorescence microscopy applied to the investigation of fibroblast cells layered on a substrate with an array of precisely spaced functionalized AuNPs: cartoon summarizing the experimental set-up. Adapted with permission from¹²³. Copyright (2014) American Chemical Society. Panel (C) Self-Assembly Formation of Lipid Membranes on Nanoplasmonic Sensor Platforms. Time-resolved extinction maximum wavelength shift measurements (red) and corresponding time derivative (blue) for vesicle adsorption onto (left) silicon oxide-coated nanodisk surface, (center) bare gold nanodisks on glass surface, and (right) titanium oxide-coated nanodisk surface. Adapted with permission from¹²⁴. Copyright (2014) WILEY-VCH Verlag GmbH & Co. KGaA, Weinheim. Panel (D) (left) Set-up of the nanoplasmonic assay for probing by eye protein contaminants (single and aggregated exogenous proteins, SAP) in EV preparations; (right) eppendorf tubes containing AuNPs in the presence of EVs (blue) or EVs + SAP (red), highlighting the sensitivity of the assay to EVs protein contaminants; UV-visible absorbance spectra of AuNPs, in the presence of increasing amounts of EVs, highlighting the sensitivity of the assay to EVs concentration. Adapted with permission from¹³⁰. Copyright (2015) American Chemical Society.

1 section 2; however, it has been demonstrated that electrostatic
 2 interactions play a major role also for neutral zwitterionic lipids
 3 facing anionic and cationic NPs^{110,111}. In addition, it has been
 4 observed that the molecular structure of membrane's lipid
 5 components (e.g. saturation degree of hydrophobic chains)
 6 represents another factor to take into account, affecting the
 7 penetration level of NPs inside the lipid region¹¹². Furthermore,
 8 cholesterol, one of the most abundant sterols in real lipid
 9 membranes, deeply affects the structure and fluidity of lipid
 10 bilayers; moreover, it is involved in the formation of lipid
 11 rafts¹¹³, which, for reasons not yet fully understood, increase
 12 the extent of NPs-membrane interactions: as an example,
 13 Melby et al.¹¹⁴ showed that positively charged AuNPs bind
 14 significantly more to phase-segregated bilayers with respect to
 15 single phase ones, while Hartono et al.¹¹⁵ associated higher
 16 cholesterol concentrations in lipid monolayers to stronger
 17 interactions with protein-coated AuNPs, leading to monolayer
 18 disruption. 73
 19 74
 20 **3.4 Biophysics of nano-bio interfaces: NPs-induced membrane** 75
 21 **modifications** 76
 22 The self-assembled nature and lateral fluidity of plasma
 23 membranes determine a capability of the membrane to
 24 reorganize and locally and transiently restructure itself in
 25 response to biological *stimuli*. This is the case considering for
 26 instance the transient formation of lipid rafts, in relationship
 27 with cell trafficking phenomena, or considering ligand (drug)
 28 receptor interactions at cell surface, triggering complex
 29 biological responses. In this respect, several studies have
 30 addressed the effects on NPs on a target lipid membrane upon
 31 adhesion. A first effect is the induced lateral phase separation
 32 within the target membrane: theoretical studies on cationic NPs
 33 have highlighted their tendency to recruit anionic lipids in the
 34 adhesion area, determining the formation of phase separated
 35 patches within the membrane (See Figure 3B).^{22,116} The
 36 alteration of membrane's phase behaviour induced by NPs is a
 37 growing research topic, with several studies contributing to
 38 building-up a complex picture, which is far from being
 39 understood. As an example, the group of Granick¹¹¹ reported a
 40 different effect of silica anionic¹¹⁷ and cationic particles on
 41 phospholipid membranes, with negative NPs inducing gelation
 42 and positive ones provoking fluidification. Considering anionic
 43 silica NPs with different size, the group of Zhang et al.¹¹⁸ reported
 44 that the gelation, or "freeze effect" on DOPC giant unilamellar
 45 vesicles (GUV) is promoted by small NPs (18 nm), while large
 46 particles (>78 nm) promote membrane wrapping, significantly
 47 decreasing the phospholipid lateral mobility, and the
 48 release of tension through stress-induced fracture mechanisms
 49 results in a microsize hole in the GUVs after interaction. On the
 50 other hand, membrane wrapping leads to increased lipid lateral
 51 mobility and the eventual collapse of the vesicles. 105
 52 Von White et al.³⁰ registered an increase in the gel-to-liquid
 53 crystalline transition temperature of synthetic lipid vesicles
 54 induced by the embedding of hydrophobic AuNPs, while
 55 Chakraborty et al.¹¹⁹ reported the opposite effect, i.e.
 56 phospholipid bilayer softening, due to hydrophobic AuNPs 109
 110

inclusions; on the other side, recent studies demonstrated that
 hydrophilic (negatively and positively charged) AuNPs induce
 the same effect at the nanoscale, promoting the formation of
 rigidified lipid domains around the NPs' surface, characterized
 by a reduced lipid motion with respect to the surrounding fluid
 phase^{21,22,120,121}. Both the induced lateral phase separation on a
 target membrane and the induced modification of the
 viscoelastic properties might represent, at the biological level,
 both biologically relevant signals, activating cell entry pathways,
 or else might be of relevance in inducing cytotoxic effects
 (Figure 3 C).

3.5 Analytical Applications of NP-lipid membrane interactions

An interesting research topic related to the interaction of NPs
 with lipid membranes is its exploitation for analytical purposes.
 Inorganic NPs are characterized by peculiar properties, making
 them suitable to provide a readout, generally an optical
 (fluorescence, scattering) or magnetic signal, which can provide
 qualitative or quantitative information of different nature.
 Knowles and coworkers have shown how the spontaneous
 formation of a supported lipid bilayer on a polystyrene NPs
 patterned support can be exploited to form membrane regions
 of high curvature, due to NPs partial wrapping: these areas
 spontaneously accumulate specific, single-tailed lipids, of
 higher spontaneous curvature, and can be exploited to monitor
 the interaction of biomolecules with membrane areas of high
 curvature¹²²; Liu et al.¹²³ have formed AuNPs patterned surfaces
 (See Figure 4B), for mechanical tension measurements in living
 cells. Cho and coworkers¹²⁴ have designed a nanoplasmonic
 biosensor made of an array of gold, silicon oxide or titanium
 oxide nanodisks coated with different lipid architectures (See
 Figure 4C), vesicles arrays, supported lipid bilayers or a
 coexistence of the two systems, spontaneously formed due to
 different pathways of interaction between lipid vesicles and the
 nanodisks of different material: localized surface plasmon
 resonance experiments detecting a membrane-active peptide
 highlighted a strong dependence of the interaction between the
 peptide and the lipid bilayer, depending on the architecture of
 the lipid scaffold. Limaj et al.¹²⁵ designed an infrared biosensor
 to monitor the molecular behaviour and dynamics of lipid
 membranes, based on the adsorption of lipid vesicles on an
 engineered substrate functionalized with gold nanoantennas
 for surface enhanced infrared absorption (SEIRA) experiments.
 Suga et al.¹²⁶ exploited the interaction of hydrophobic
 (dodecanthiol-modified) AuNPs with phospholipids and
 phospholipid assemblies, to investigate the behavior of lipid
 membranes at a molecular length-scale through Surface-
 Enhanced Raman Spectroscopy (SERS). The same technique is
 employed by Bhowmik et al.¹²⁷, who exploit the formation of a
 lipid coating wrapping Silver NPs (AgNPs) to probe through SERS
 the molecular behavior of protein oligomers spontaneously
 binding to the lipid coating of AgNPs (this example will be also
 discussed in section 5) (See Figure 4A). Recently, we have shown
 that synthetic Giant Unilamellar Vesicles of POPC promote the

1 clusterization of Turkevich-Frens citrated AuNPs on the lipid
 2 membrane itself¹²¹. This phenomenon, which has been
 3 investigated by other groups, provokes a modification of the
 4 plasmon resonance peak of AuNPs, which is visible also by
 5 naked eyes as a colour change of AuNPs dispersion from red to
 6 blue^{17,128}. Interestingly, this effect is similarly observed when
 7 the same AuNPs challenge biogenic natural vesicles
 8 (extracellular vesicles, EVs)^{120,129} and it has been found as
 9 strongly dependent on the concentration of EVs and on the
 10 presence of protein contaminant. Therefore, an analytical
 11 method for EVs has been developed, offering an easy and fast
 12 assay for purity and concentration of EVs, based on nonspecific
 13 interactions between NPs and lipid membranes^{130–132} (see
 14 Figure 4D).

15 4. Engineering Lipid Assemblies: Inclusion of NPs 16 in Lipid Scaffolds

17 Depending on their molecular structure and on the
 18 environmental conditions, lipids in water self-assemble into
 19 very diverse structures, from simple planar lamellar phases,
 20 vesicles, to non-lamellar curved bilayered structures (as cubic
 21 mesophases)^{133–135}, to inverse monolayered tubular
 22 arrangements (as inverse hexagonal mesophases). These
 23 different structural arrangements, formed by spontaneous self-
 24 assembly, can host hydrophilic-coated NPs in the aqueous
 25 regions and/or hydrophobic-coated NPs in the hydrophobic
 26 domains.
 27 NPs can spontaneously insert in the lipid scaffolds, due to non-
 28 specific forces, such as hydrophobic, electrostatic and Van der
 29 Waals interactions (see paragraph 2), thus representing a facile
 30 approach to obtain a complex hybrid material with controlled
 31 structure and defined properties arising from the combination
 32 of lipid and NP building blocks.
 33 In particular, the inclusion of NPs in lipid scaffolds allows
 34 obtaining materials with specific interesting features: (i) the
 35 biocompatibility of the lipid scaffold (dependent on its
 36 composition) allows envisioning the employment of these
 37 hybrid materials for biomedical applications; (ii) the self-
 38 organization and phase behavior of lipid mesophases are
 39 generally responsive to the inclusion of external species, such
 40 as temperature, hydration and other experimental conditions,
 41 which variations can be triggered, in a space and time controlled
 42 manner, by external *stimuli* applied to the NPs included in the
 43 lipid scaffold (e.g., magnetoliposomes). This is a very interesting
 44 opportunity for several applications, for instance the controlled
 45 development of drug delivery systems (DDS) with controlled
 46 release abilities; (iii) the inclusion and confinement of NPs in
 47 lipid scaffolds has the effect to locally concentrate them and
 48 impose them a spatial arrangement. This localized NP
 49 concentration increase might be of relevance to enhance NP-
 50 related signals (for instance optical or MRI readout for
 51 diagnostic applications); in addition, the increased NP
 52 concentration, together with a defined structural architecture,
 53 might induce peculiar collective properties of NPs, arising from
 54 the lipid scaffold-imposed arrangement.

In the following sections we will revise this topic, in particular
 focusing on the effect of NPs inclusion on the overall features of
 lipid/NP hybrid materials (4.1), and, subsequently, on
 applicative examples of NP/lipid hybrids made of NPs included
 in lamellar (4.2) and non-lamellar (4.3) lipid mesophases.

4.1 NPs inclusion in Lipid Scaffolds: Structural and Physicochemical Effects

The hydrophobic or hydrophilic nature of NPs, which depends
 on the coating agent, is the key factor in determining the
 localization in a lipid assembly. Both lamellar (i.e. liposomes,
 Giant Unilamellar Vesicles) and non-lamellar (i.e. cubic or
 hexagonal structures) lipid assemblies are characterized by the
 coexistence of hydrophobic and hydrophilic domains, capable
 to host NPs of different nature. In all NPs-lipid hybrids, the
 inclusion of NPs in the lipid architecture affects the physico-
 chemical and structural properties of the lipid scaffold,
 modifying for instance the fluidity and bending properties of the
 membrane, its local thickness, the phase behavior and the
 viscoelastic properties. For instance, it has been shown that the
 inclusion of hydrophobic superparamagnetic iron oxide NPs
 (SPIONs) in the lipid membrane of DPPC liposomes increases the
 average thickness of the membrane and modifies the
 orientation of the phospholipid chains, affecting the lipid
 melting temperature^{136,137}. In addition, depending on the
 chemical nature of hydrophobic NPs embedded in a lipid
 bilayer, they can either stabilize or destabilize the lipid ordering,
 causing opposite effects on the phase behavior of the lipid
 scaffold; it has been shown that 4 and 5.7 nm AgNPs³¹ increase
 the fluidity of the membrane, reducing the degree of ordering
 of the lipid tails, while 5 nm maghemite NPs²⁹ increase
 membrane rigidity. Finally, the inclusion of nanoparticles can
 also modify the final structure of the bilayer: for instance, a
 Cryo-TEM investigation of Chen et al. on liposomes containing
 hydrophobic SPIONs has highlighted the formation of
 liposomes' aggregates with SPIONs clusters acting as bridging
 agents (See Figure 5A-B). These local perturbations highlight
 that some structural rearrangement of a planar lipid membrane
 can be possible preserving the overall lipid mesophase
 architecture; however, as reported by Briscoe et al.⁴⁰,
 significant amounts of NPs inclusion might promote, for defined
 lipid compositions and specific temperature/pressure
 conditions, a phase transition from lamellar to hexagonal
 mesophases. In general, as already pointed out in section 2, the
 inclusion of NPs in a planar bilayer increases the frustration
 packing energy of the lipid molecules eventually promoting the
 re-organization in a different mesophase, characterized by a
 more negative curvature; the mismatch between the
 equilibrium curvature and the perturbed arrangement due to
 NP inclusion, favors the transition to a more thermodynamically
 stable structure.

These examples highlight how the effect of NPs on lipid
 membranes is variable, but possibly predictable, on the basis of
 minimum energy considerations; therefore, the physico-
 chemical properties of the target lipid membrane and of the NPs
 to be inserted in the lipid scaffold can be tuned in order to

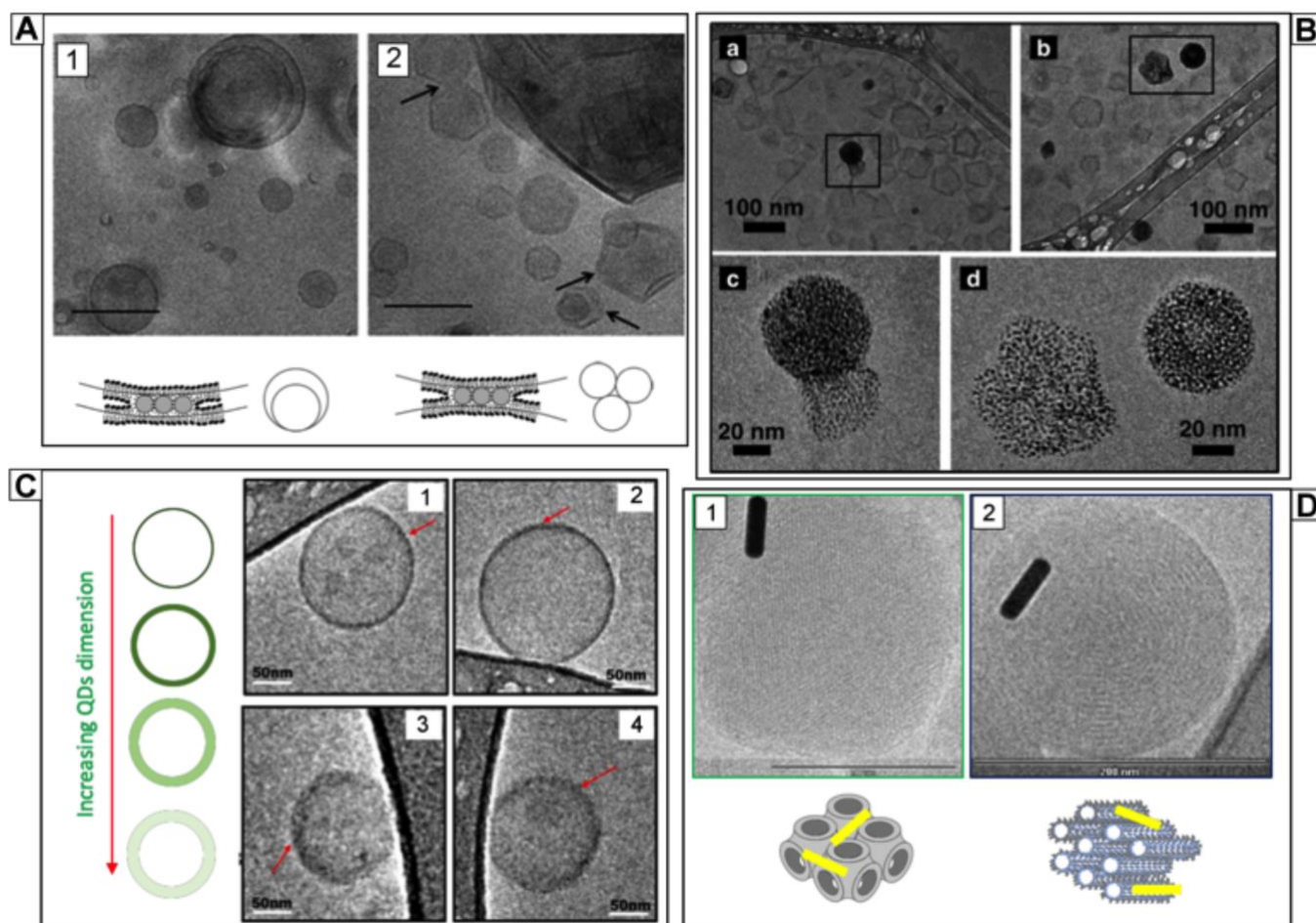


Figure 5 Cryo-Microscopies of Lamellar and Non-Lamellar Lipid membranes assembled with hydrophobic NPs. *Panel (A)* Cryo-TEM images highlighting the structural changes induced by hydrophobic SPIONs interacting with liposomes: on the left, TEM image showing liposomes arranged in a multiwalled configuration with SPIONs bridging; on the right, TEM image of liposomes' aggregates bridged by SPIONs clusters embedded in the bilayer. Adapted with permission from Ref.²⁹. Copyright (2010) American Chemical Society. *Panel (B)* DPPC liposomes decorated with dodecanethiol-capped AuNPs shown at different magnifications. Adapted with permission from Ref.²⁸. Copyright (2017) American Chemical Society. *Panel (C)* TEM images of POPC/POPE liposomes assembled with Quantum Dots (QDs) of different sizes embedded in the bilayer. The size increase of QDs (from 1 to 4 progressively) increases the perturbation of the lipid membrane: lipid membrane appears sharp when small QDs are included (1 and 2), while with the larger ones the membrane becomes fuzzier (3 and 4). Reproduced from Ref.¹⁵⁰ with permission from The Royal Society of Chemistry. *Panel (D)* Cryo-SEM of Non-Lamellar mesophases interacting with Au NRs. On the left Phytantriol cubic mesophase, on the right Phytantriol hexagonal mesophase, both assembled with Au NRs. Adapted with permission from Ref.¹⁵⁶. Copyright (2012) American Chemical Society.

1 modify the behavior of the membrane in a desired manner¹⁹
 2 engineering the system for its final purpose.²⁰
 3
 4 **4.2 Applications of NPs/Lamellar Lipid Assemblies Hybrids**²²
 5 Among hybrid nanostructures where NPs are included in²³
 6 lamellar assemblies, particularly relevant are²⁴
 7 magnetoliposomes (MLs), where hydrophobic SPIONs are²⁵
 8 included in the lipid bilayers of lipid vesicles^{138–140}. Their²⁶
 9 responsivity to static (SMF) and alternating magnetic fields²⁷
 10 (AMF) makes MLs good candidates in nanomedicine as DDS¹⁴¹
 11 able to release drugs confined in the lumen of liposomes in a²⁹
 12 time and space controlled manner, upon application of external³⁰
 13 stimuli^{142,143}. Despite their potentiality, the inclusion of small³¹
 14 NPs in the bilayer can be exploited only for drug delivery³²
 15 purposes, while generally, no bulk heating effect can be induced³³
 16 by small NPs subjected to AMFs, as shown in several studies¹⁴⁴
 17 therefore, they cannot be applied in hyperthermia therapies³⁵
 18 for the thermal ablation of cells; however, as reported by³⁶
 37

Corato et al.¹⁴⁵, using hydrophilic SPIONs loaded in the vesicles' lumen combined with a photosensitizer, results in a synergistic effect, observed both *in vitro* and *in vivo*, making this strategy, exploiting a multifunctional nanomaterial, very promising for therapeutic applications. Recently, MLs decorated both with hydrophobic and hydrophilic SPIONs have been shown to release on-demand hydrophilic or hydrophobic payloads, depending on the frequency and application time of an AMF.¹²⁷ Besides SPIONs, hydrophobic AuNPs were recently used¹⁴⁶ to build-up photoresponsive and thermosensitive hybrid liposomes. In addition, multifunctional hybrid liposomes containing magneto-plasmonic nanoparticles (SPIONs@Au), merging the possibility to combine hypothermic and photothermal treatments were recently shown^{147,148} for image-guided delivery of anti-HIV drugs to the brain: generally, the successful delivery of antiretroviral drugs to the brain is limited due to the presence of the blood–brain barrier (BBB); in this case the authors reported an enhanced BBB transmigration efficiency under AMF without its disruption; moreover, the

1 treatment of HIV virus with multifunctional liposomes
 2 successfully reduced the viral replication. 58
 3 Several studies have addressed the inclusion of quantum dots
 4 in lipid assemblies: despite their unique optical properties, they
 5 are characterized by significant acute cytotoxic effects. With the
 6 aim to realize a contrast agent for imaging applications^{138,149,150}
 7 several studies have shown that the confinement of CdSe dots
 8 in lipid bilayers increases their biocompatibility, while
 9 preserving their fluorescence features, making the system more
 10 suitable for biomedical applications (See Figure 5 C). 66
 11 67
 12 **4.3 Applications of NPs/Non-Lamellar Lipid Assemblies Hybrids** 68
 13 As anticipated in section 2, the inclusion of NPs into non-
 14 lamellar lipid assemblies mostly affects the structure of the
 15 mesophase, in terms of the lattice parameter and
 16 consequently, of the diameter of the nanochannels and amount
 17 of water contained in the lipid architecture. If the size of NPs is
 18 similar or smaller than the lattice parameter, NPs can be easily
 19 encapsulated in the architectures. Venugopal et al.³⁸
 20 investigated the encapsulation of hydrophilic Silica NPs of 8 nm
 21 diameter in monolinolein mesophase: in this case, the NPs
 22 were too large to be encapsulated in the nanochannels (of
 23 3.8 nm diameter); nevertheless, the addition of NPs determined
 24 the overall dehydration of the lipid scaffold, eventually causing
 25 for high concentration, the transition of the assembly geometry
 26 to a gyroid cubic structure (Ia3d). The authors interpret this
 27 behavior considering that, since the energy cost to include the
 28 NPs in the nanochannels is extremely high (above 100 k_BT), the
 29 NPs tend to minimize their interfacial energy, aggregating along
 30 the grain boundaries of the mesophase, similarly to what
 31 reported concerning lamellar structures¹⁵¹. The same authors
 32 investigated also the structural features of monolinolein
 33 mesophases loaded with hydrophilic SPIONs. Upon application
 34 of a SMF, a reorganization of the lipid domains along the
 35 direction of the field^{152,153} was found, highlighting how the
 36 responsiveness of SPIONs to magnetic fields can be exploited to
 37 induce structural modifications in the whole lipid mesophase.
 38 This effect has been applied for instance to control the release
 39 of drugs confined in the lipid mesophases¹⁵² or, as the same
 40 authors reported¹⁵⁴, for the application in optical memory
 41 storage. 95
 42 The inclusion of hydrophobic NPs in non-lamellar mesophases
 43 can be easily achieved exploiting the hydrophobic interactions
 44 that spontaneously drive the NPs localization in the
 45 hydrophobic regions of the self-assembly. However, also in this
 46 case, the size of NPs is of paramount importance, to avoid the
 47 disruption of the lipid scaffold. Recently, the inclusion
 48 of hydrophobic SPIONs into 1-monoolein diamond cubic phase
 49 was reported, highlighting that the amount of included NPs,
 50 together with temperature, control the phase transition from
 51 cubic to hexagonal phase. Since this transition is accompanied
 52 by a significant dehydration of the mesophase, the structural
 53 rearrangement is accompanied by the release of most of the
 54 water content of the nanochannels. This thermoresponsive
 55 hybrid material was also found to be responsive to AMF,
 56 representing, therefore, a promising system for the delivery of

hydrophilic drugs in a time and space-controlled manner.³³
 Recently, it was shown that this thermotropic effect of liquid
 crystalline phases loaded with hydrophobic NPs is a general
 phenomenon, highlighted e.g. also by cubic mesophases
 formed of phytantriol and hydrophobic AuNPs.²⁰
 Very few examples in the literature address the inclusion of
 non-spherical NPs in non-lamellar lipid assemblies: Boyd et al.¹⁵⁵
 reported on hydrophobic NRs included in phytantriol, selachyl
 alcohol and monoolein lipid mesophases, with the aim to build-
 up photo-responsive hybrid materials (See Figure 5D). The
 authors investigate the effect of NRs on the cubic mesophases,
 highlighting a slight reduction in the phase transition
 temperature and in the lattice parameter. Interestingly,
 similarly to spherical hydrophobic NPs, gold NRs shift the cubic-
 to-hexagonal boundaries to lower temperature¹⁵⁶. For
 hexosomes of selachyl alcohol, it was shown that the lattice
 parameter or water volume fraction^{26,27} are not affected by the
 presence of AuNRs; the authors suggest that NRs are positioned
 along the direction of hexosomes, but, due to their large sizes
 (55.5 nm in length and 16 nm in width) they are in close
 proximity of the lipid bilayer, without being efficiently included
 inside it. Nevertheless, the application of a NIR laser on the
 hybrid structure promoted the phase transition from cubic to
 hexagonal phase, similarly to what observed with the
 application of AMF on monoolein-SPIONs hybrids.

5. Surface Engineering of Inorganic NPs: Functionalization of NPs with a Lipid Coating

Recently, several research groups have addressed the
 functionalization of inorganic NPs or clusters of NPs with lipids
 to form lipid-coated NPs with a supported lipid bilayer (SLB and
 liposomes³). The validity of this approach is twofold: first, a lipid
 coating of appropriate composition might strongly improve the
 biocompatibility of inorganic NPs: this is particularly critical for
 the very toxic quantum dots. The second advantage is the
 increased dispersibility in body fluids and improved
 pharmacokinetic properties. As a matter of fact, without a
 proper coating, bare NPs introduced by parenteral
 administration, are rapidly opsonized and removed by
 phagocytes from the blood stream⁵⁴ and accumulated in liver
 and spleen^{157,158}, often causing oxidative stress^{159,160}.

Although this could be even convenient for those treatments
 where the desired aim is to modulate local immune
 responses¹⁶¹, it is worth considering the use of a capping agent
 that prevents leakage of the drug, protects the carrier from
 degrading enzymes, and shields them from the immune system
 avoiding side effects^{162,163}. Among several potential capping
 systems, lipid bilayers are especially advantageous¹⁶⁴ for several
 reasons: (i) the escape from endosomal vesicles of the
 nanomaterial and successful reaching of its biological target,
 upon endocytic uptake, is strongly favoured in the presence of
 a lipid coating, improving the ability of NPs to passively
 permeate to the inner core of the cell^{165,166}; (ii) the presence of
 a lipid coating is helpful in preventing NPs aggregation in
 biological environment; (iii) lipid coating is highly tuneable in

1 composition (for instance PEGylated lipids, to further improve
2 nanoparticle pharmacokinetic properties¹⁶⁷, can be easily
3 incorporated, as well as cholesterol, added as a controlling
4 fluidity agent) and can be easily functionalized and designed to
5 match the specific requirements of the desired application¹⁶⁹
6 ¹⁷⁰. As introduced in section 2, the achievement of such a
7 coating depends on the size of the NP to be coated and on the
8 viscoelastic properties of the membrane. Generally, relatively
9 large NPs, imposing a low curvature to the target membrane
10 can be successfully completely wrapped and coated by a lipid
11 membrane, while small particles need to be wrapped and
12 coated as clusters. In the following sections we will review
13 the most relevant examples and applications of lipid-coated
14 inorganic nanoparticles, considering one by one the different
15 types of nanoparticles, Silica NPs (5.1), Gold and Silver NPs (5.2)
16 and Iron Oxide NPs (5.3).

17
18 **5.1 Lipid-coated Silica NPs**

19 Leveraging the pioneering works of Rapuano's groups^{171,172}, over
20 the last years several research groups have addressed the
21 decoration of silica nanoparticles with SLBs¹⁷³. Recently
22 Mousseau et al. showed an example of fluorescent silica NPs
23 covered by a pulmonary surfactant Curosurf®. They found that
24 a complete SLB coverage of silica nanoparticles is obtained only
25 through sonication, which disrupts lipid vesicles and promotes

full wrapping of the NPs. *In vitro* assays confirmed that the
presence of the SLB mitigated the particle toxicity and improved
internalization rates¹⁷⁴.

Tada and co-workers tested the impact of a lipid coating (using
different types of lipid bilayers) on the cytolocalization of silica
NPs prepared with methylene blue, for applications in
Photodynamic Therapy (PDT)^{175,176}.

Mackowiak et al.¹⁷⁷ showed an example of mesoporous silica
NPs surrounded by a cationic DOPC/DOTAP SLB with targeting
ligands on the surface of the nanoconstruct and a
photosensitizer molecule covalently attached to the surface of
mesoporous silica NPs, for controlled and targeted drug
delivery applications. In this case, the presence of the SLB
coating was also aimed at improving the capability of the system
to retain a drug inside the mesoporous structure of NPs before
photoactivation to induce the release of the cargo.

An alternative route to obtain controlled release of drugs from
lipid-coated mesoporous silica NPs, based on the use of thermo-
responsive lipids, was recently presented by Zhang et al.: they
combined the high drug loading capacity of mesoporous silica
NPs with the thermal responsiveness of a mixture of lipids,
DPPC/DSPC/Chol/DSPE-PEG2000, allowing the possibility to
release on-demand the payload at hyperthermia temperature,
circumventing the premature leakage at physiological
temperature¹⁷⁸ (See Figure 6C).

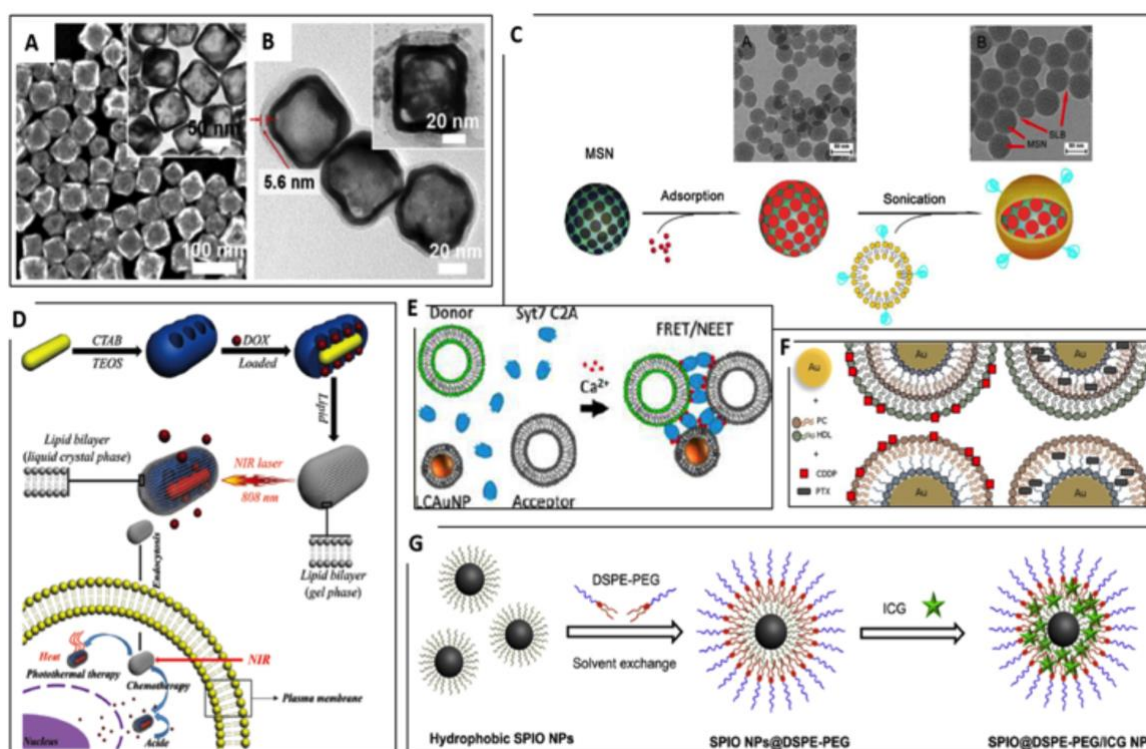


Figure 6 Lipid-coated NPs. Panel (A-B) TEM images of bare Au nanocages (A) and the same nanocages covered by a lipid bilayer (B) used as nanovaccine for cancer immunotherapy. Reprinted with permission from ref.¹⁸⁷ © Elsevier; Panel (C) Schematic overview of the procedure for the fabrication of doxorubicin (DOX)-loaded SLB-mesoporous silica NPs. The thermal responsiveness of the lipids circumvents the premature leakage of the payload. The insets show the related TEM images. Adapted and reprinted with permission from ref.¹⁷⁸ © Elsevier; Panel (D) Schematic illustration of the fabrication process of DOX-AuNR@mSiO₂ covered by a lipid bilayer and the corresponding NIR laser-controlled intracellular DOX release. Reprinted with permission from ref.¹⁹² © RSC; Panel (E) Model of the Ca²⁺-dependent liposome and lipid-coated AuNPs clustering in presence of synaptotagmin (SyT). Reprinted with permission from ref.¹⁸⁵ © ACS; Panel (F) Conceptual scheme of lipid-coated gold carriers for the release of paclitaxel and cisplatin. Reprinted with permission from ref.¹⁸³ © Elsevier; Panel (G) Schematic illustration of the preparation protocol of SPIO@DSPE-PEG loaded with indocyanine green. Reprinted with permission from ref.¹⁹³ © Elsevier.

1
 2 **5.2 Lipid-coated Gold and Silver NPs**
 3 Taking advantage of their antimicrobial properties, AgNPs have
 4 been widely used in the last decades both in industrial and in
 5 biomedical application^{179–181}. Furthermore, due the localized
 6 surface plasmon resonance (LSPR) of AgNPs, they can be
 7 exploited for the development of biosensors. For this purpose,
 8 Bhowmik et al.¹²⁷ developed a method to determine the
 9 conformation of membrane-bound proteins: unlike
 10 conventional SERS, that requires immobilization of molecules
 11 they exploit the spontaneous binding of proteins to lipid bilayer
 12 coated AgNPs. In this way, they probed the behavior of
 13 membrane-attached oligomers of Amyloid- β 40 (A β 40), whose
 14 conformation is of relevance in Alzheimer's disease. AuNPs are
 15 the most widely studied inorganic NPs, thanks to their facile
 16 synthetic and functionalization routes, and their plasmon
 17 properties that can be harnessed in a plethora of applications
 18 ranging from optical imaging, spectroscopy and photothermal
 19 therapy. Du et al. formed a liposomes-AuNPs hybrid system
 20 a vector for nucleic acids, for applications in gene therapy¹⁸².
 21 England and co-workers^{183,184} (See Figure F) prepared AuNPs
 22 functionalized with multiple layers (two or three) of
 23 phosphatidylcholine, alkanethiol, high density lipoprotein and
 24 phosphatidylcholine/alkanethiol for the delivery of
 25 hydrophobic and hydrophilic drugs for the treatment of solid
 26 tumours. By exploiting the optical properties of AuNPs, Reed
 27 et al. developed a novel hybrid for sensitive detection of proteins
 28 based on apposition and aggregation of liposomes induced by
 29 Ca^{2+} ions using Forster resonance energy transfer (FRET)
 30 assays¹⁸⁵ (See Figure E). Wang et al. recently proposed a novel
 31 approach to overcome the low delivery efficiency of plasmids
 32 by condensing them on peptide-modified AuNPs, successively
 33 covered with a mixture of phospholipids¹⁸⁶.
 34 In addition to spherical NPs, liposomes-coated gold
 35 nanocages¹⁸⁷ (See Figure 6A-B) have been reported as possible
 36 nanovaccines for cancer immunotherapy: the authors
 37 demonstrated that the hybrid carrier exhibited enhanced
 38 antitumor effects, inhibiting tumour growth in lung metastasis
 39 models. In addition, lipid-coated hollow gold nanoshells have
 40 been recently developed for synergistic chemotherapy and
 41 photothermal therapy for the treatment of pancreatic
 42 cancer¹⁸⁸. By taking advantage of the unique structure of hollow
 43 gold nanoshells, the authors successfully demonstrated the
 44 delivery of two drugs, one loaded in the lipid bilayer and the
 45 other one loaded in the hydrophilic interior of the nanoshell.
 46 Furthermore, the possibility to extend lipid coverage to Au NRs
 47 has been recently explored. Recent studies have addressed the
 48 functionalization of Au NRs with a phospholipid bilayer
 49 composed of POPC¹⁸⁹ and, more recently, DMPC¹⁹⁰, to increase
 50 biocompatibility and bioavailability of NRs. In addition, lipid
 51 capped Au NRs (obtained with DPPC vesicles containing lipids
 52 with a thiol headgroup) have been demonstrated to be suitable
 53 label-free biosensors¹⁹¹ for the detection of lipophilic drugs
 54 aqueous solutions or lipopeptides in serum. Finally, moving to
 55 more complex architecture, Han et al.¹⁹² (See Figure 6D)
 56 demonstrated the possibility to use silica and phospholipids to

cover Au NRs, coupling the photothermal and thermo-responsive properties in the same nanoplatform.

5.3 Lipid-coated Iron Oxide NPs

SPIONs are among the most attractive NPs for biomedical applications, ranging from applications in MRI to responsive nanocarriers for drug delivery to therapeutic applications in hyperthermia (See Figure G). Bao et al.¹⁹³ synthesized DSPE-PEG coated SPIONs loaded with indocyanine green molecules as superparamagnetic carriers capable to easily accumulate in tumours sites and act as biodegradable nanotheranostic agents. In the emerging field of nanovaccines, the group of Ruiz-de-Angulo¹⁹⁴ presented a biocompatible multifunctional system designed to both act as delivery vehicle and radiotracer for PET/SPECT imaging: using lipid-coated magnetite nanoparticles, they efficiently included in the construct $^{67}\text{Ga}^{3+}$ as radiotracer, plus an antigen and an adjuvant. *In vivo* imaging highlighted the efficient targeting capability of the system and cell uptake. Recently, the same authors presented bacteria-mimicking NPs, that is, a similar construct (i.e., lipid coated magnetite nanoparticles), coated with lipooligosaccharides, which efficiently act as adjuvants¹⁹⁵ for application in cancer vaccine field.

Enveloping a magnetic iron oxide core with a lipid shell facilitates bioconjugation, biocompatibility, and delivery, as well reported by Wang et al.¹⁹: in their work they provide a general solution for coating iron oxide and other metal oxides with a simple mixing in water, facilitating applications in biosensing, separation, and nanomedicine.

A multifunctional system for dual imaging (fluorescence and MRI) of hepatocellular carcinoma was reported by Liang et al.¹⁹⁶: through the thin film hydration method, they covered magnetite NPs previously conjugated with a NIR fluorescent dye; the lipid bilayer was decorated with a polymer targeting tumour hepatocytes, able to steer the carrier to the specific site. By flow cytometry and confocal laser scanning microscopy they assessed the specific cellular uptake, followed by *in vivo* tests on tumor-bearing mice.

6. Conclusions

In this contribution we have reviewed the latest developments concerning the interaction of NPs with amphiphilic bilayers arranged in lamellar and non-lamellar mesophases.

This area is a very lively research field, where efforts are motivated by several scientific purposes. First of all, the application of nanostructured materials in the biomedical field requires a precise knowledge of the nano-bio-interface: bilayered synthetic assemblies are a very convenient and simple platform to elucidate the interactions with cell membranes and internalization of nanomedical devices. In addition, the design of smart nanostructured hybrid devices, where NPs are included in soft matter assemblies to contribute new properties and modulate their phase diagram is a very relevant and active research field. Related to this latter area is the use of lipid

- 1 bilayers as coating shells for inorganic nanoparticles, to improve
2 their biocompatibility and interaction with cell membranes. 52
3 In all cases, the mechanistic understanding of the main
4 thermodynamic parameters involved in this interaction and
5 their dependence on the physico-chemical features both of NPs
6 and of the bilayers, are a necessary prerequisite to engineer soft
7 matter hybrids and formulate NPs with potential applications
8 the biomedical field. Soft Matter science represents therefore
9 the central discipline, whose scientific and methodological
10 approaches will be more and more pivotal to contribute to
11 meaningful progresses in this field. If the promises held by this
12 approach will be fulfilled in the next decades, many of the
13 current hurdles that nowadays hamper the full development of
14 nanomedicine can be overcome. 64
15 Finally, a precise knowledge of the above-mentioned features
16 allows engineering NPs to probe the properties of complex
17 bilayer assemblies, both of natural and synthetic origin. This
18 a very exciting and promising area, where fundamental and
19 applied efforts should be directed in the next decade. 69
70
20 **Conflicts of interest** 71
21 There are no conflicts to declare 72
73
22 **Acknowledgements** 74
23 Costanza Montis acknowledges the European Union's Horizon
24 2020 programme (evFOUNDRY grant agreement 801367). All
25 the authors thank CSGI for financial support. 79
80
26 **References** 81
27 1 C. Lu, Y. Liu, Y. Ying and J. Liu, *Langmuir*, 2017, **33**, 630–
28 637. 84
29 2 P.-J. J. Huang, F. Wang and J. Liu, *Langmuir*, 2016, **32**,
30 2458–2463. 86
31 3 X. Wang, X. Li, H. Wang, X. Zhang, L. Zhang, F. Wang and J.
32 Liu, *Langmuir*, 2019, **35**, 1672–1681. 88
33 4 F. Wang and J. Liu, *J. Am. Chem. Soc.*, 2015, **137**, 11736–
34 11742. 90
35 5 F. Wang and J. Liu, *Nanoscale*, 2013, **5**, 12375. 91
36 6 Y. Liu and J. Liu, *Nanoscale*, 2017, **9**, 13187–13194. 92
37 7 V. C. Sanchez, A. Jachak, R. H. Hurt and A. B. Kane, *Chem.*
38 *Res. Toxicol.*, 2012, **25**, 15–34. 94
39 8 R. Koole, M. M. van Schooneveld, J. Hilhorst, K.
40 Castermans, D. P. Cormode, G. J. Strijkers, C. de Mello
41 Donegá, D. Vanmaekelbergh, A. W. Griffioen, K. Nicolay, Z.
42 A. Fayad, A. Meijerink and W. J. M. Mulder, *Bioconjug.*
43 *Chem.*, 2008, **19**, 2471–2479. 100
44 9 A. H. Bahrami, M. Raatz, J. Agudo-Canalejo, R. Michel, E.
45 Curtis, C. K. Hall, M. Gradzielski, R. Lipowsky and T. R.
46 Weigl, *Adv. Colloid Interface Sci.*, 2014, **208**, 214–224. 102
47 10 S. Dasgupta, T. Auth and G. Gompper, *J. Phys. Condens.*
48 *Matter*, 2017, **29**, 373003. 104
49 11 X. Chen, F. Tian, X. Zhang and W. Wang, *Soft Matter*, 2013,
50 **9**, 7592. 106
12 Y. Roiter, M. Ornatska, A. R. Rammohan, J. Balakrishnan, D.
13 R. Heine and S. Minko, *Nano Lett.*, 2008, **8**, 941–944.
14 C. Contini, M. Schneemilch, S. Gaisford and N. Quirke, *J.*
15 *Exp. Nanosci.*, 2018, **13**, 62–81.
16 Q. Mu, G. Jiang, L. Chen, H. Zhou, D. Fourches, A. Tropsha
17 and B. Yan, *Chem. Rev.*, 2014, **114**, 7740–7781.
18 S. Dasgupta, T. Auth and G. Gompper, *Nano Lett.*, 2014, **14**,
19 687–693.
20 A. H. Bahrami, *Soft Matter*, 2013, **9**, 8642.
21 F. Wang and J. Liu, *Nanoscale*, 2015, **7**, 15599–15604.
22 F. Wang, D. E. Curry and J. Liu, *Langmuir*, 2015, **31**, 13271–
23 13274.
24 F. Wang, X. Zhang, Y. Liu, Z. Y. W. Lin, B. Liu and J. Liu,
25 *Angew. Chemie Int. Ed.*, 2016, **55**, 12063–12067.
26 X. Liu, X. Li, W. Xu, X. Zhang, Z. Huang, F. Wang and J. Liu,
27 *Langmuir*, 2018, **34**, 6628–6635.
28 J. Liu, *Langmuir*, 2016, **32**, 4393–4404.
29 T. Pfeiffer, A. De Nicola, C. Montis, F. Carlà, N. F. A. van der
30 Vegt, D. Berti and G. Milano, *J. Phys. Chem. Lett.*, 2019, **10**,
31 129–137.
32 M. Schulz, A. Olubummo and W. H. Binder, *Soft Matter*,
33 2012, **8**, 4849.
34 C. F. Su, H. Merlitz, H. Rabbel and J. U. Sommer, *J. Phys.*
35 *Chem. Lett.*, 2017, **8**, 4069–4076.
36 R. C. Van Lehn and A. Alexander-Katz, *Soft Matter*, 2014,
37 **10**, 648–658.
38 M. Mendoza, C. Montis, L. Caselli, M. Wolf, P. Baglioni and
39 D. Berti, *Nanoscale*, 2018, **10**, 3480–3488.
40 M. Mendoza, L. Caselli, C. Montis, S. Orazzini, E. Carretti,
41 P. Baglioni and D. Berti, *J. Colloid Interface Sci.*, 2019, **541**,
42 329–338.
43 M. R. Preiss, A. Hart, C. Kitchens and G. D. Bothun, *J. Phys.*
44 *Chem. B*, 2017, **121**, 5040–5047.
45 Y. Chen, A. Bose and G. D. Bothun, *ACS Nano*, 2010, **4**,
46 3215–3221.
47 G. Von White, Y. Chen, J. Roder-Hanna, G. D. Bothun and C.
48 L. Kitchens, *ACS Nano*, 2012, **6**, 4678–4685.
49 G. D. Bothun, *J. Nanobiotechnology*, 2008, **6**, 1–10.
50 Z. A. Almsherqi, T. Landh, S. D. Kohlwein and Y. Deng, in
International Review of Cell and Molecular Biology, Elsevier
Inc., 1st edn., 2009, vol. 274, pp. 275–342.
D. P. Chang, J. Barauskas, A. P. Dabkowska, M. Wadsäter, F.
Tiberg and T. Nylander, *Adv. Colloid Interface Sci.*, 2015,
222, 135–147.
W. K. Fong, R. Negrini, J. J. Vallooran, R. Mezzenga and B. J.
Boyd, *J. Colloid Interface Sci.*, 2016, **484**, 320–339.
I. W. Hamley, *Angew. Chemie*, 2003, **115**, 1730–1752.
G. C. Shearman, O. Ces, R. H. Templer and J. M. Seddon, *J.*
Phys. Condens. Matter, 2006, **18**, S1105–S1124.
C. M. Beddoes, C. P. Case and W. H. Briscoe, *Adv. Colloid*
Interface Sci., 2015, **218C**, 48–68.
E. Venugopal, S. K. Bhat, J. J. Vallooran and R. Mezzenga,
Langmuir, 2011, **27**, 9792–9800.
M. Slezak, D. Nieciecka, A. Joniec, M. Pękala, E. Gorecka,
M. Emo, M. J. Stébé, P. Krysiński and R. Bilewicz, *ACS Appl.*
Mater. Interfaces, 2017, acsami.6b12889.
J. M. Bulpett, T. Snow, B. Quignon, C. M. Beddoes, T.-Y. D.

- 1 Tang, S. Mann, O. Shebanova, C. L. Pizzey, N. J. Terrill, S. A58
2 Davis and W. H. Briscoe, *Soft Matter*, 2015, **11**, 8789–80059 63
3 41 C. M. Beddoes, J. Berge, J. E. Bartenstein, K. Lange, A. J. 60
4 Smith, R. K. Heenan and W. H. Briscoe, *Soft Matter*, 2016, **61**
5 **12**, 6049–6057. 62 64
6 42 C. Montis, B. Castroflorio, M. Mendoza, A. Salvatore, D. 63
7 Berti and P. Baglioni, *J. Colloid Interface Sci.*, 2015, **449**, 64 65
8 317–326. 65
9 43 K. L. Chen and G. D. Bothun, *Environ. Sci. Technol.*, 2014, **66**
10 **48**, 873–880. 67
11 44 M. Henriksen-Lacey, S. Carregal-Romero and L. M. Liz- 68
12 Marzán, *Bioconjug. Chem.*, 2017, **28**, 212–221. 69
13 45 E. Rascol, J.-M. Devoisselle and J. Chopineau, *Nanoscale*, 70
14 2016, **8**, 4780–4798. 71
15 46 E. Blanco, H. Shen and M. Ferrari, *Nat. Biotechnol.*, 2015, **72**
16 **33**, 941–951. 73
17 47 P. Falagan-Lotsch, E. M. Grzincic and C. J. Murphy, *Proc.* 74
18 *Natl. Acad. Sci.*, 2016, **113**, 13318–13323. 75
19 48 C. J. Murphy, A. M. Vartanian, F. M. Geiger, R. J. Hamers, 76
20 Pedersen, Q. Cui, C. L. Haynes, E. E. Carlson, R. Hernandez 77
21 R. D. Klapser, G. Orr and Z. Rosenzweig, *ACS Cent. Sci.*, 2017, **3**
22 **1**, 117–123. 79
23 49 L. J. Fox, R. M. Richardson and W. H. Briscoe, *Adv. Colloid* 80
24 *Interface Sci.*, 2018, **257**, 1–18. 81
25 50 S. Wilhelm, A. J. Tavares, Q. Dai, S. Ohta, J. Audet, H. F. 82
26 Dvorak and W. C. W. Chan, *Nat. Rev. Mater.*, 2016, **1**, 83
27 16014. 84
28 51 D. Bobo, K. J. Robinson, J. Islam, K. J. Thurecht and S. R. 85
29 Corrie, *Pharm. Res.*, 2016, **33**, 2373–2387. 86
30 52 Y. H. Choi and H. K. Han, *J. Pharm. Investig.*, 2018, **48**, 43–87
31 60. 88
32 53 J. M. Caster, A. N. Patel, T. Zhang and A. Wang, *Wiley* 89
33 *Interdiscip. Rev. Nanomedicine Nanobiotechnology*, , 90
34 DOI:10.1002/wnan.1416. 91
35 54 C. D. Walkey and W. C. W. Chan, *Chem. Soc. Rev.*, 2012, **41**, 92
36 2780–2799. 93
37 55 A. E. Nel, L. Mädler, D. Velegol, T. Xia, E. M. V. Hoek, P. 94
38 Somasundaran, F. Klaessig, V. Castranova and M. 95
39 Thompson, *Nat. Mater.*, 2009, **8**, 543–557. 96
40 56 S. Zhang, H. Gao and G. Bao, *ACS Nano*, 2015, **9**, 8655– 97
41 8671. 98
42 57 N. S. Bhise, J. Ribas, V. Manoharan, Y. S. Zhang, A. Polini, 99
43 Massa, M. R. Dokmeci and A. Khademhosseini, *J. Control* 100
44 *Release*, 2014, **190**, 82–93. 101
45 58 G. Rossi and L. Monticelli, *Biochim. Biophys. Acta -* 102
46 *Biomembr.*, 2016, **1858**, 2380–2389. 103
47 59 V. Pillay, K. Murugan, Y. E. Choonara, P. Kumar, D. 104
48 Bijukumar and L. C. du Toit, *Int. J. Nanomedicine*, 2015, **10**, 105
49 2191. 106
50 60 I. Canton and G. Battaglia, *Chem. Soc. Rev.*, 2012, **41**, 27107
51 61 M. Calero, L. Gutiérrez, G. Salas, Y. Luengo, A. Lázaro, P. 108
52 Acedo, M. P. Morales, R. Miranda and A. Villanueva, 109
53 *Nanomedicine Nanotechnology, Biol. Med.*, 2014, **10**, 73310
54 743. 111
55 62 S. Behzadi, V. Serpooshan, W. Tao, M. A. Hamaly, M. Y. 112
56 Alkawareek, E. C. Dreaden, D. Brown, A. M. Alkilany, O. 113
57 Farokhzad and M. Mahmoudi, *Chem. Soc. Rev.*, 2017, **46**, 114
4218–4244.
Y. Jiang, S. Huo, T. Mizuhara, R. Das, Y. W. Lee, S. Hou, D. F.
Moyano, B. Duncan, X. J. Liang and V. M. Rotello, *ACS*
Nano, 2015, **9**, 9986–9993.
K. A. Dawson, A. Lesniak, F. Fenaroli, M. P. Monopoli, A.
Christoffer and A. Salvati, *ACS Nano*, 2012, 5845–5857.
J. Blechinger, A. T. Bauer, A. A. Torrano, C. Gorzelanny, C.
Bräuchle and S. W. Schneider, *Small*, 2013, **9**, 3970–3980.
S. Tatur, M. MacCarini, R. Barker, A. Nelson and G.
Fragneto, *Langmuir*, 2013, **29**, 6606–6614.
C. Montis, V. Generini, G. Boccalini, P. Bergese, D. Bani and
D. Berti, *J. Colloid Interface Sci.*, 2018, **516**, 284–294.
E. Fröhlich, *Int. J. Nanomedicine*, 2012, **7**, 5577–5591.
J. A. Yang, S. E. Lohse and C. J. Murphy, *Small*, 2014, **10**,
1642–1651.
E. Lee, H. Jeon, M. Lee, J. Ryu, C. Kang, S. Kim, J. Jung and Y.
Kwon, *Sci. Rep.*, 2019, **9**, 2494.
Y. C. Park, J. B. Smith, T. Pham, R. D. Whitaker, C. A. Sucato,
J. A. Hamilton, E. Bartolak-Suki and J. Y. Wong, *Colloids*
Surfaces B Biointerfaces, 2014, **119**, 106–114.
J. Lin, H. Zhang, V. Morovati and R. Dargazany, *J. Colloid*
Interface Sci., 2017, **504**, 325–333.
K. P. García, K. Zarschler, L. Barbaro, J. A. Barreto, W.
O'Malley, L. Spiccia, H. Stephan and B. Graham, *Small*,
2014, **10**, 2516–2529.
L. Zhang, H. Xue, C. Gao, L. Carr, J. Wang, B. Chu and S.
Jiang, *Biomaterials*, 2010, **31**, 6582–6588.
N. Gal, A. Lassenberger, L. Herrero-Nogareda, A. Scheberl,
V. Charwat, C. Kasper and E. Reimhult, *ACS Biomater. Sci.*
Eng., 2017, **3**, 249–259.
E. Giovanelli, E. Muro, G. Sitbon, M. Hanafi, T. Pons, B.
Dubertret and N. Lequeux, *Langmuir*, 2012, **28**, 15177–
15184.
K. Kaaki, K. Hervé-Aubert, M. Chiper, A. Shkilnyy, M. Soucé,
R. Benoit, A. Paillard, P. Dubois, M. L. Saboungi and I.
Chourpa, *Langmuir*, 2012, **28**, 1496–1505.
A. Kraus, L. Wortmann, L. Hermanns, N. Feliu, M. Vahter, S.
Stucky, S. Mathur and B. Fadeel, *Nanomedicine*
Nanotechnology, Biol. Med., 2014, **10**, 1421–1431.
X. Wang, X. Wang, X. Bai, L. Yan, T. Liu, M. Wang, Y. Song,
G. Hu, Z. Gu, Q. Miao and C. Chen, *Nano Lett.*, 2019, **19**, 8–
18.
P. Vedantam, G. Huang and T. R. J. Tzeng, *Cancer*
Nanotechnol., 2013, **4**, 13–20.
B. Pelaz, G. Charron, C. Pfeiffer, Y. Zhao, J. M. De La Fuente,
X. J. Liang, W. J. Parak and P. Del Pino, *Small*, 2013, **9**,
1573–1584.
M. P. Monopoli, D. Walczyk, A. Campbell, G. Elia, I. Lynch,
F. Baldelli Bombelli and K. a Dawson, *J. Am. Chem. Soc.*,
2011, **133**, 2525–2534.
F. Bertoli, D. Garry, M. P. Monopoli, A. Salvati and K. A.
Dawson, *ACS Nano*, 2016, **10**, 10471–10479.
S. Milani, F. Baldelli Bombelli, A. S. Pitek, K. a Dawson and J.
Rädler, *ACS Nano*, 2012, **6**, 2532–2541.
G. Caracciolo, O. C. Farokhzad and M. Mahmoudi, *Trends*
Biotechnol., 2017, **35**, 257–264.
A. Lesniak, A. Salvati, M. J. Santos-Martinez, M. W.

- 1 Radomski, K. a. Dawson and C. Åberg, *J. Am. Chem. Soc.*, 2013, **135**, 1438–1444. 58
- 2 2013, **135**, 1438–1444. 59
- 3 87 D. Hühn, K. Kantner, C. Geidel, S. Brandholt, I. De Cock, S. 60
- 4 H. Soenen, P. Riveragil, J. M. Montenegro, K. Braeckmans 61
- 5 K. Müllen, G. U. Nienhaus, M. Klapper and W. J. Parak, *ACS* 62
- 6 *Nano*, 2013, **7**, 3253–3263. 63
- 7 88 W. Lin, T. Insley, M. D. Tuttle, L. Zhu, D. A. Berthold, P. Kra 64
- 8 C. M. Rienstra and C. J. Murphy, *J. Phys. Chem. C*, 2015, 65
- 9 **119**, 21035–21043. 66
- 10 89 C. C. Fleischer and C. K. Payne, *Acc. Chem. Res.*, 2014, **47**, 67
- 11 2651–2659. 68
- 12 90 F. Wang, L. Yu, M. P. Monopoli, P. Sandin, E. Mahon, A. 69
- 13 Salvati and K. A. Dawson, *Nanomedicine Nanotechnology*, 70
- 14 *Biol. Med.*, 2013, **9**, 1159–1168. 71
- 15 91 L. Treuel, S. Brandholt, P. Maffre, S. Wiegele, L. Shang and 72
- 16 G. U. Nienhaus, *ACS Nano*, 2014, **8**, 503–513. 73
- 17 92 S. Fogli, C. Montis, S. Paccosi, A. Silvano, E. Michelucci, D. 74
- 18 Berti, A. Bosi, A. Parenti and P. Romagnoli, *Nanomedicine* 75
- 19 2017, **12**, 1647–1660. 76
- 20 93 R. P. Carney, T. M. Carney, M. Mueller and F. Stellacci, 77
- 21 *Biointerphases*, 2012, **7**, 17. 78
- 22 94 F. Simonelli, D. Bochicchio, R. Ferrando and G. Rossi, *J.* 79
- 23 *Phys. Chem. Lett.*, 2015, **6**, 3175–3179. 80
- 24 95 S. Li and N. Malmstadt, *Soft Matter*, 2013, **9**, 4969. 81
- 25 96 A. M. Farnoud and S. Nazemidashtarjandi, *Environ. Sci.* 82
- 26 *Nano*, 2019, **6**, 13–40. 83
- 27 97 A. Šarić and A. Cacciuto, *Soft Matter*, 2013, **9**, 6677–6695 84
- 28 98 K. Jaskiewicz, A. Larsen, D. Schaeffel, K. Koynov, I. 85
- 29 Lieberwirth, G. Fytas, K. Landfester and A. Kroeger, *ACS* 86
- 30 *Nano*, 2012, **6**, 7254–7262. 87
- 31 99 A. Šarić and A. Cacciuto, *Phys. Rev. Lett.*, 2012, **108**, 88
- 32 118101. 89
- 33 100 H. Zhang, Q. Ji, C. Huang, S. Zhang, B. Yuan, K. Yang and Y 90
- 34 Q. Ma, *Sci. Rep.*, 2015, **5**, 10525. 91
- 35 101 M. Raatz, R. Lipowsky and T. R. Weikl, *Soft Matter*, 2014, 92
- 36 **10**, 3570–3577. 93
- 37 102 A. H. Bahrami, R. Lipowsky and T. R. Weikl, *Phys. Rev. Lett.* 94
- 38 2012, **109**, 188102. 95
- 39 103 N. D. Burrows, A. M. Vartanian, N. S. Abadeer, E. M. 96
- 40 Grzincic, L. M. Jacob, W. Lin, J. Li, J. M. Dennison, J. G. 97
- 41 Hinman and C. J. Murphy, *J. Phys. Chem. Lett.*, 2016, **7**, 98
- 42 632–641. 99
- 43 104 S. Nangia and R. Sureshkumar, *Langmuir*, 2012, **28**, 17660 100
- 44 17671. 101
- 45 105 R. Vácha, F. J. Martinez-Veracochea and D. Frenkel, *Nano* 102
- 46 *Let.*, 2011, **11**, 5391–5395. 103
- 47 106 Y. Qiu, Y. Liu, L. Wang, L. Xu, R. Bai, Y. Ji, X. Wu, Y. Zhao, 104
- 48 Li and C. Chen, *Biomaterials*, 2010, **31**, 7606–7619. 105
- 49 107 A. Espinosa, A. K. A. Silva, A. Sánchez-Iglesias, M. Grzelczak 106
- 50 C. Péchoux, K. Desboeufs, L. M. Liz-Marzán and C. Wilhelm 107
- 51 *Adv. Healthc. Mater.*, 2016, **5**, 1040–1048. 108
- 52 108 H. I. Ingólfsson, M. N. Melo, F. J. Van Eerden, C. Arnarez 109
- 53 A. Lopez, T. A. Wassenaar, X. Periole, A. H. De Vries, D. P. 110
- 54 Tieleman and S. J. Marrink, *J. Am. Chem. Soc.*, 2014, **136**, 111
- 55 14554–14559. 112
- 56 109 T. Lunnoo, J. Assawakhajornsak and T. Puangmali, *J. Phys.* 113
- 57 *Chem. C*, 2019, **123**, 3801–3810. 114
- M. Laurencin, T. Georgelin, B. Malezieux, J. M. Siaugue and 110
- C. Ménager, *Langmuir*, 2010, **26**, 16025–16030.
- B. Wang, L. Zhang, S. C. Bae and S. Granick, *Proc. Natl.* 111
- Acad. Sci.*, 2008, **105**, 18171–18175.
- G. D. Bothun, N. Ganji, I. A. Khan, A. Xi and C. Bobba, 112
- Langmuir*, 2017, **33**, 353–360.
- T. Róg, M. Pasenkiewicz-Gierula, I. Vattulainen and M. 113
- Karttunen, *Biochim. Biophys. Acta - Biomembr.*, 2009,
- 1788, 97–121.
- E. S. Melby, A. C. Mensch, S. E. Lohse, D. Hu, G. Orr, C. J. 114
- Murphy, R. J. Hamers and J. A. Pedersen, *Environ. Sci.*
- Nano*, 2016, **3**, 45–55.
- D. Hartono, Hody, K. L. Yang and L. Y. Lanry Yung, 115
- Biomaterials*, 2010, **31**, 3008–3015.
- F. Lolicato, L. Joly, H. Martinez-Seara, G. Fragneto, E. 116
- Scoppola, F. Baldelli Bombelli, I. Vattulainen, J. Akola and
- M. Maccarini, *Small*, 2019, **15**, 1805046.
- R. Michel, E. Kesselman, T. Plostica, D. Danino and M. 117
- Gradzielski, *Angew. Chemie Int. Ed.*, 2014, **53**, n/a-n/a.
- S. Zhang, A. Nelson and P. A. Beales, *Langmuir*, 2012, **28**, 118
- 12831–12837.
- S. Chakraborty, A. Abbasi, G. D. Bothun, M. Nagao and C. L. 119
- Kitchens, *Langmuir*, 2018, **34**, 13416–13425.
- C. Montis, A. Zandrini, F. Valle, S. Busatto, L. Paolini, A. 120
- Radeghier, A. Salvatore, D. Berti and P. Bergese, *Colloids*
- Surfaces B Biointerfaces*, 2017, **158**, 331–338.
- C. Montis, D. Maiolo, I. Alessandri, P. Bergese and D. Berti, 121
- Nanoscale*, 2014, **6**, 6452–6457.
- J. C. Black, P. P. Cheney, T. Campbell and M. K. Knowles, 122
- Soft Matter*, 2014, **10**, 2016–2023.
- Y. Liu, R. Medda, Z. Liu, K. Galior, K. Yehl, J. P. Spatz, E. A. 123
- Cavalcanti-Adam and K. Salaita, *Nano Lett.*, 2014, **14**,
- 5539–5546.
- G. H. Zan, J. A. Jackman, S.-O. Kim and N.-J. Cho, *Small*, 124
- 2014, **10**, 4828–4832.
- O. Limaj, D. Etezadi, N. J. Wittenberg, D. Rodrigo, D. Yoo, S. 125
- H. Oh and H. Altug, *Nano Lett.*, 2016, **16**, 1502–1508.
- K. Suga, T. Yoshida, H. Ishii, Y. Okamoto, D. Nagao, M. 126
- Konno and H. Umakoshi, *Anal. Chem.*, 2015, **87**, 4772–
- 4780.
- D. Bhowmik, K. R. Mote, C. M. MacLaughlin, N. Biswas, B. 127
- Chandra, J. K. Basu, G. C. Walker, P. K. Madhu and S. Maiti,
- ACS Nano*, 2015, **9**, 9070–9077.
- K. Sugikawa, T. Kadota, K. Yasuhara and A. Ikeda, *Angew.* 128
- Chemie - Int. Ed.*, 2016, **55**, 4059–4063.
- C. Montis, S. Busatto, F. Valle, A. Zandrini, A. Salvatore, Y. 129
- Gerelli, D. Berti and P. Bergese, *Adv. Biosyst.*, 2018, **2**,
- 1700200.
- D. Maiolo, L. Paolini, G. Di Noto, A. Zandrini, D. Berti, P. 130
- Bergese and D. Ricotta, *Anal. Chem.*, 2015, **87**, 4168–4176.
- S. Busatto, A. Giacomini, C. Montis, R. Ronca and P. 131
- Bergese, *Anal. Chem.*, 2018, **90**, 7855–7861.
- A. Mallardi, N. Nuzziello, M. Liguori, C. Avolio and G. 132
- Palazzo, *Colloids Surfaces B Biointerfaces*, 2018, **168**, 134–
- 142.
- J. Zhai, C. Fong, N. Tran and C. J. Drummond, *ACS Nano*, 133
- 2019, **13**, acsnano.8b07961.

- 1 134 R. Mezzenga, J. M. Seddon, C. J. Drummond, B. J. Boyd, *G58*
 2 E. Schröder-Turk and L. Sagalowicz, *Adv. Mater.*, 2019, **59**
 3 **1900818**, 1–19. **60**
- 4 135 H. M. G. Barriga, M. N. Holme and M. M. Stevens, *Angew.
 5 Chemie Int. Ed.*, 2019, **58**, 2958–2978. **62**
- 6 136 A. Salvatore, C. Montis, D. Berti and P. Baglioni, *ACS Nano*,
 7 2016, **10**, 7749–7760. **64**
- 8 137 O. Bixner and E. Reimhult, *J. Colloid Interface Sci.*, 2016, **65**
 9 **466**, 62–71. **66**
- 10 138 R. Martínez-González, J. Estelrich and M. A. Busquets, *Int.
 11 Mol. Sci.*, 2016, **17**, 1–14. **68**
- 12 139 B. Drasler, P. Budime Santhosh, D. Drobne, M. Erdani Kreft,
 13 S. Kralj, D. Makovec and N. Poklar Ulrih, *Int. J.
 14 Nanomedicine*, 2015, **10**, 6089. **71**
- 15 140 S. Saesoo, S. Sathornsumetee, P. Anekwiang, C.
 16 Treetidnipa, P. Thuwajit, S. Bunthot, W. Maneeprakorn,
 17 Maurizi, H. Hofmann, R. U. Rungsardthong and N.
 18 Saengkrit, *Colloids Surfaces B Biointerfaces*, 2018, **161**,
 19 497–507. **76**
- 20 141 E. Amstad, J. Kohlbrecher, E. Müller, T. Schweizer, M.
 21 Textor and E. Reimhult, *Nano Lett.*, 2011, **11**, 1664–1670. **78**
- 22 142 S. Nappini, S. Fogli, B. Castroflorio, M. Bonini, F. Baldelli
 23 Bombelli and P. Baglioni, *J. Mater. Chem. B*, 2016, **4**, 716–
 24 725. **81**
- 25 143 J. Haša, J. Hanuš and F. Štěpánek, *ACS Appl. Mater.
 26 Interfaces*, 2018, **10**, 20306–20314. **83**
- 27 144 P. Pradhan, J. Giri, F. Rieken, C. Koch, O. Mykhaylyk, M.
 28 Döblinger, R. Banerjee, D. Bahadur and C. Plank, *J. Control.
 29 Release*, 2010, **142**, 108–121. **86**
- 30 145 R. Di Corato, G. Béalle, J. Kolosnjaj-Tabi, A. Espinosa, O.
 31 Clément, A. K. A. Silva, C. Ménager and C. Wilhelm, *ACS*
 32 *Nano*, 2015, **9**, 2904–2916. **89**
- 33 146 A. K. Rengan, A. B. Bukhari, A. Pradhan, R. Malhotra, R.
 34 Banerjee, R. Srivastava and A. De, *Nano Lett.*, 2015, **15**,
 35 842–848. **92**
- 36 147 A. Tomitaka, H. Arami, Z. Huang, A. Raymond, E. Rodriguez,
 37 Y. Cai, M. Febo, Y. Takemura and M. Nair, *Nanoscale*, 2018,
 38 **10**, 184–194. **95**
- 39 148 M. E. Khosroshahi, *J. Nanomed. Nanotechnol.*,
 40 DOI:10.4172/2157-7439.1000298. **97**
- 41 149 R. B. Lira, M. A. B. L. Seabra, A. L. L. Matos, J. V.
 42 Vasconcelos, D. P. Bezerra, E. De Paula, B. S. Santos and
 43 Fontes, *J. Mater. Chem. B*, 2013, **1**, 4297–4305. **100**
- 44 150 M. Wlodek, M. Kolasinska-Sojka, M. Szuwarzynski, S.
 45 Kereiche, L. Kovacic, L. Zhou, L. Islas, P. Warszynski and
 46 H. Briscoe, *Nanoscale*, 2018, **10**, 17965–17974. **103**
- 47 151 J. B. Marlow, M. J. Pottage, T. M. McCoy, L. De Campo,
 48 Sokolova, T. D. M. Bell and R. F. Tabor, *Phys. Chem. Chem.
 49 Phys.*, 2018, **20**, 16592–16603. **106**
- 50 152 J. J. Vallooran, R. Negrini and R. Mezzenga, *Langmuir*, 2017,
 51 **29**, 999–1004. **108**
- 52 153 J. J. Vallooran, S. Handschin, S. Bolisetty and R. Mezzenga,
 53 *Langmuir*, 2012, **28**, 5589–5595. **110**
- 54 154 J. J. Vallooran, S. Bolisetty and R. Mezzenga, *Adv. Mater.*
 55 2011, **23**, 3932–3937. **112**
- 56 155 W. K. Fong, T. L. Hanley, B. Thierry, A. Tilley, N. Kirby, L.
 57 Waddington and B. J. Boyd, *Phys. Chem. Chem. Phys.*, 2011,
13, 24936–24953. **114**
- 156 W. K. Fong, T. L. Hanley, B. Thierry, N. Kirby, L. J.
 Waddington and B. J. Boyd, *Langmuir*, 2012, **28**, 14450–
 14460.
- 157 S. M. Moghimi, A. C. Hunter and T. L. Andresen, *Annu. Rev.
 Pharmacol. Toxicol.*, 2011, **52**, 481–503.
- 158 S. Mitragotri and J. Lahann, *Adv. Mater.*, 2012, **24**, 3717–
 3723.
- 159 W. H. De Jong, W. I. Hagens, P. Krystek, M. C. Burger, A. J.
 A. M. Sips and R. E. Geertsma, *Biomaterials*, 2008, **29**,
 1912–1919.
- 160 P. Aggarwal, J. B. Hall, C. B. McLeland, M. A. Dobrovolskaia
 and S. E. McNeil, *Adv. Drug Deliv. Rev.*, 2009, **61**, 428–437.
- 161 T. A. Wynn, A. Chawla and J. W. Pollard, *Nature*, 2013, **496**,
 445–55.
- 162 B. Illes, P. Hirschle, S. Barnert, V. Cauda, S. Wuttke and H.
 Engelke, *Chem. Mater.*, 2017, **29**, 8042–8046.
- 163 K. Raemdonck, K. Braeckmans, J. Demeester and S. C. De
 Smedt, *Chem. Soc. Rev.*, 2014, **43**, 444–472.
- 164 A. Luchini and G. Vitiello, *Front. Chem.*, 2019, **7**, 1–16.
- 165 M. E. Davis, Z. Chen and D. M. Shin, *Nat. Rev. Drug Discov.*,
 2008, **7**, 771–782.
- 166 N. Kamaly, Z. Xiao, P. M. Valencia, A. F. Radovic-Moreno
 and O. C. Farokhzad, *Chem. Soc. Rev.*, 2012, **41**, 2971.
- 167 Z. Shen, H. Ye, M. Kröger and Y. Li, *Phys. Chem. Chem.
 Phys.*, 2017, **19**, 13294–13306.
- 168 A. Luchini, R. K. Heenan, L. Paduano and G. Vitiello, *Phys.
 Chem. Chem. Phys.*, 2016, **18**, 18441–18449.
- 169 T. M. Allen and P. R. Cullis, *Adv. Drug Deliv. Rev.*, 2013, **65**,
 36–48.
- 170 E. Terreno, F. Uggeri and S. Aime, *J. Control. Release*, 2012,
161, 328–337.
- 171 R. Rapuano and A. M. Carmona-Ribeiro, *J. Colloid Interface
 Sci.*, 1997, **193**, 104–111.
- 172 R. Rapuano and A. M. Carmona-Ribeiro, *J. Colloid Interface
 Sci.*, 2000, **226**, 299–307.
- 173 A. L. Troutier and C. Ladavière, *Adv. Colloid Interface Sci.*,
 2007, **133**, 1–21.
- 174 F. Mousseau, C. Puisney, S. Mornet, R. Le Borgne, A.
 Vacher, M. Airiau, A. Baeza-Squiban and J. F. Berret,
Nanoscale, 2017, **9**, 14967–14978.
- 175 L. M. Rossi, P. R. Silva, L. L. R. Vono, A. U. Fernandes, D. B.
 Tada and M. S. Baptista, *Langmuir*, 2008, **24**, 12534–12538.
- 176 D. B. Tada, E. Suraniti, L. M. Rossi, C. A. P. Leite, C. S.
 Oliveira, T. C. Tumolo, R. Calemczuk, T. Livache and M. S.
 Baptista, *J. Biomed. Nanotechnol.*, 2014, **10**, 519–528.
- 177 S. A. Mackowiak, A. Schmidt, V. Weiss, C. Argyo, C. Von
 Schirnding, T. Bein and C. Bräuchle, *Nano Lett.*, 2013, **13**,
 2576–2583.
- 178 Q. Zhang, X. Chen, H. Shi, G. Dong, M. Zhou, T. Wang and
 H. Xin, *Colloids Surfaces B Biointerfaces*, 2017, **160**, 527–
 534.
- 179 S. Chernousova and M. Epple, *Angew. Chemie - Int. Ed.*,
 2013, **52**, 1636–1653.
- 180 R. R. Arvizo, S. Bhattacharyya, R. A. Kudgus, K. Giri, R.
 Bhattacharya and P. Mukherjee, *Chem. Soc. Rev.*, 2012, **41**,
 2943.

- 1 181 L. Cheng, M. D. Weir, H. H. K. Xu, J. M. Antonucci, N. J. Lin,
2 S. Lin-Gibson, S. M. Xu and X. Zhou, *J. Biomed. Mater. Res.*
3 *Part B Appl. Biomater.*, 2012, **100B**, 1378–1386.
- 4 182 B. Du, L. Tian, X. Gu, D. Li, E. Wang and J. Wang, *Small*,
5 2015, **11**, 2333–2340.
- 6 183 C. G. England, A. M. Gobin and H. B. Frieboes, *Eur. Phys. J.*
7 *Plus*, 2015, **130**, 231.
- 8 184 H. Frieboes, C. England, T. Priest, G. Zhang, X. Sun, D. Patel,
9 L. McNally, V. van Berkel and A. Gobin, *Int. J.*
10 *Nanomedicine*, 2013, 3603.
- 11 185 D. J. Hamilton, M. D. Coffman, J. D. Knight and S. M. Reed,
12 *Langmuir*, 2017, **33**, 9222–9230.
- 13 186 P. Wang, L. Zhang, W. Zheng, L. Cong, Z. Guo, Y. Xie, L.
14 Wang, R. Tang, Q. Feng, Y. Hamada, K. Gonda, Z. Hu, X. Wu
15 and X. Jiang, *Angew. Chemie - Int. Ed.*, 2018, **57**, 1491–
16 1496.
- 17 187 R. Liang, J. Xie, J. Li, K. Wang, L. Liu, Y. Gao, M. Hussain, G.
18 Shen, J. Zhu and J. Tao, *Biomaterials*, 2017, **149**, 41–50.
- 19 188 B. K. Poudel, B. Gupta, T. Ramasamy, R. K. Thapa, S. Pathak,
20 K. T. Oh, J. H. Jeong, H. G. Choi, C. S. Yong and J. O. Kim,
21 *Colloids Surfaces B Biointerfaces*, 2017, **160**, 73–83.
- 22 189 C. J. Orendorff, T. M. Alam, D. Y. Sasaki, B. C. Bunker and J.
23 A. Voigt, *ACS Nano*, 2009, **3**, 971–983.
- 24 190 P. B. Santhosh, N. Thomas, S. Sudhakar, A. Chadha and E.
25 Mani, *Phys. Chem. Chem. Phys.*, 2017, **19**, 18494–18504.
- 26 191 E. T. Castellana, R. C. Gamez and D. H. Russell, *J. Am. Chem.*
27 *Soc.*, 2011, **133**, 4182–4185.
- 28 192 X. Cui, W. Cheng and X. Han, *J. Mater. Chem. B*, 2018, **6**,
29 8078–8084.
- 30 193 Y. Ma, S. Tong, G. Bao, C. Gao and Z. Dai, *Biomaterials*,
31 2013, **34**, 7706–7714.
- 32 194 A. Ruiz-De-Angulo, A. Zabaleta, V. Gómez-Vallejo, J. Llop
33 and J. C. Mareque-Rivas, *ACS Nano*, 2016, **10**, 1602–1618.
- 34 195 G. Traini, A. Ruiz-de-Angulo, J. B. Blanco-Canosa, K.
35 Zamacola Bascarán, A. Molinaro, A. Silipo, D. Escors and J.
36 C. Mareque-Rivas, *Small*, , DOI:10.1002/sml.201803993.
- 37 196 J. Liang, X. Zhang, Y. Miao, J. Li and Y. Gan, *Int. J.*
38 *Nanomedicine*, 2017, **12**, 2033–2044.
- 39 197 A. Torchi, F. Simonelli, R. Ferrando and G. Rossi, *ACS Nano*,
40 2017, **11**, 12553–12561.
- 41